Mechanistic basis of lung cancer prevention with green tea catechins focused on anti-tumor immunity

ANCHALEE RAWANGKAN

15DB053

A Thesis Submitted in Partial Fulfillment of the Requirements for the Degree of Doctor of Philosophy

Supervisor: Professor Masami Suganuma

Department of Life Science

Graduate School of Science and Engineering

Saitama University

JAPAN

September 2018

ABSTRACT

Green tea catechin, (-)-epigallocatechin gallate (EGCG), and green tea are well known effective non-toxic cancer preventives. To understand the mechanisms of action of EGCG that results in wide beneficial effects on cancer prevention, I studied whether EGCG enhances anti-tumor immunity by focusing on the immune checkpoint. Programmed cell death-ligand 1 (PD-L1) in tumor cells is an immune checkpoint molecule involved in immune evasion of tumor: It inhibits the immune response of T cells by binding to PD-1 on T cells. The PD-L1 expression is induced by cytokines and growth factors in the inflammatory tumor microenvironment. In this thesis, I studied the effects of EGCG on inducible PD-L1 expression in human lung cancer cells, and the stimulation of T-cell functions, examined by the model experiment using tumor specific cluster of differentiation 3 positive (CD3+) T cells co-cultured with F10-OVA cells.

First, I found that PD-L1 protein levels varied among human lung cancer cell lines: Lu99 cells showed the highest PD-L1 expression, A549 cells were moderate, and H1299 were very low. Treatment with interferon gamma (IFN-γ) increased cell-surface PD-L1 level in A549 and H1299 cells as determined by flow cytometry, but not in Lu99 cells. However, treatment with epidermal growth factor (EGF) increased PD-L1 expression in Lu99 cells. Pretreatment with EGCG and green tea extract (GTE) for 3 h dose-dependently reduced IFN-γ-induced PD-L1 mRNA and cell-surface PD-L1 level in A549 and H1299 cells by inhibiting phosphorylation of STAT1. EGCG also inhibited EGF-induced PD-L1 expression by inhibiting the AKT pathway in Lu99 cells.

Next, I examined the relationship between inhibition of PD-L1 expression and lung cancer prevention. The intraperitoneal injection of 4-(methylnitrosamino)-1-(3-pyridyl)-1-butanone (NNK) induced lung tumors in 100% A/J mice in 16 weeks and oral

administration of 0.3% GTE reduced the number of tumors per mouse from 4.1 to 2.6. In addition, the percentage of positive PD-L1 cells in tumors in NNK + GTE group was reduced from 9.6 to 2.9 (70% reduction).

Finally, I studied whether EGCG enhances anti-tumor immunity. I performed an *ex vivo* co-culture experiment using tumor specific CD3+ T cells with F10-OVA cells, to determine restoration of T cells activity: Pretreatment with EGCG reduced PD-L1 mRNA level in F10-OVA cells, and it increased IL-2 mRNA expression 1.7-fold. However, EGCG had no effect in non-co-cultured T cells. According to the reduction of PD-L1 by EGCG, apoptosis of F10-OVA cells was increased 3-fold by co-culture with tumor specific CD3+ T cells.

This is the first finding to show that EGCG and green tea extract act as alternative immune checkpoint inhibitors. This new function of EGCG in anti-tumor immune response plays a vital role in cancer prevention and enhancement of anti-cancer activities.

ACKNOWLEDGEMENTS

First, I would like to express my gratitude to my advisor Dr. Masami Suganuma, for her continuous support of my Ph.D. study and related research, and also for her patience, motivation, and immense knowledge. Her guidance made possible my research and writing of this thesis. I cannot imagine having a better advisor and mentor for my Ph.D. study, and I hope that one day I will become as good an advisor to my students as Prof. Masami Suganuma has been to me.

Besides my advisor, I would like to thank Prof. Emeritus. Drs. Hirota Fujiki and Maitree Suttajit for their insightful comments and encouragement, and also for their questions, which encouraged me to widen my research from various perspectives. I also thank the review committee members, Assoc. Prof. Drs. Shinji Tsukahara, Ichiro Sakata and Hiroshi Yoshikawa for their invaluable advice and suggestions.

I also express my gratitude to my fellow labmates for stimulating discussions, for the sleepless nights we worked together before deadlines, and for all the fun we have had in the last three years. Furthermore, I am grateful to Ms. Miki Kanno, Kaori Suzuki and Ikuko Shiotani for their scientific advice. Without their precious support, it would not have been possible to conduct this research. In addition, I convey my thanks to Dr. Takehiko Kamijo, MD, and all his colleagues at the Research Institute for Clinical Oncology, Saitama Cancer Center. Moreover, I am also grateful to Assist. Prof. Drs. Duangkamol Kunthalert and Phanchana Sanguansermsri, DVM, for their enlightening me the first glance at research.

Last but not least, I thank my family: my parents including my father who passed away after fighting esophageal cancer during my studies — a very sad time — and my older sister, niece, nephew and my partner for supporting me spiritually throughout writing this thesis, and in my life in general.

I take this opportunity to express my special gratitude to the Ministry of Education, Culture, Sports, Science and Technology (MEXT), Japan, for awarding me the Monbukagakusho scholarship, which enabled me to pursue my studies here in Japan.

ANCHALEE RAWANGKAN

Saitama, Japan

TABLE OF CONTENTS

LIST OF FIGURES

Supplemental Figure 1.

Lu99 cells expressed high CKLF Like MARVEL 89 Transmembrane Domain Containing 6 (CMTM6) mRNA expression

Chapter 1

General introduction and objectives

1.1. Research background

1.1.1. Characteristics of green tea and green tea catechins

Green tea or Sencha is the most popular daily beverage brewing tea leaves with warm water for almost 800 years in Japan. Green tea plant belongs to *Camellia sinensis* L., O. Kuntze, Theaceae family [1]. The major constituents of green tea are polyphenols, including phenolic acids (caffeic acid and gallic acid) and flavonoid. Catechins from green tea belong to the family of flavonoids containing flavan-3-ol unit and galloylated catechin [2]. Green tea catechins are characterized by the presence of a benzopyran structure bearing at least one aromatic ring (Figure 1). One Japanese size cup (120 ml) of green tea contains about 150 mg catechins, which include main four catechins (10-15% (-)-epigallocatechin gallate (EGCG), 6-10% (-)-epigallocatechin (EGC), 2-3% (-)-epicatechin gallate (ECG), and 2% (-)-epicatechin (EC). The minor green tea catechins include (-)-catechin, (-)-catechin gallate, (-)-gallocatechin, and (-)-gallocatechin gallate as shown in Figure 1 [1]. Sencha has the highest content of tea polyphenols whereas partially oxidized and fermented oolong tea has lower content, and fermented black tea contain more theaflavins and thearubigins than cathechins and polyphenols [2].

Normally, not exceeding 1 μM EGCG reached in plasma within 2 h after drinking of green tea and cleared from the blood with a half-life of 5 h in humans. Oral administration of 525 and 1600 mg EGCG of green tea extract reached 4.4 and 7.4 μM EGCG in plasma, respectively. EGCG is present mainly in the free form about 80% in plasma, whereas other catechins are highly conjugated with glucuronic acid and/or sulfate

groups. Moreover, EGCG has a wide range of target organs by distributed throughout the body including the digestive tract, blood, brain, liver, kidney, and spleen. Green tea catechins are metabolized to glucuronidation, sulfation, methylation, and ring-fission by hepatic and intestinal enzymes, and intestinal microorganism normal flora. EGCG is mainly excreted through the bile into the feces, whereas EGC, ECG, and EC are excreted through both bile and urine [2]. Therefore, green tea catechins might accumulate in the organs and induce cancer preventive effects through multi-mechanism of action in the cells after drinking a lot of green tea.

1.1.2. Cancer preventive activity of EGCG and green tea extract (GTE) in rodents

Green tea catechins are well-known non-toxic cancer preventives. In 1983, Fujiki H and Suganuma M began to study green tea within the program of cancer chemoprevention in Japan. The term "cancer chemoprevention" defined as "prevention of the occurrence of cancer by administration of one or more compounds" was coined by Sporn M B in 1976. To look for Japanese original cancer preventive agents, they studied various tannins or polyphenols including EGCG derived from medicinal plants in collaboration with Okuda T at Okayama University. Based on their study of tumor promotion, they thought that inhibitors of tumor promotion were suitable for cancer prevention rather than inhibitors of initiation. So, they found that EGCG inhibited ^{3}H-12-*O*-tetradecanoylphorbol-13-acetate (^{3}H-TPA) binding to phorbol ester receptor, and dose-dependently inhibited activation of protein kinase C [3,4,5].

In 1987, cancer preventive activity of EGCG in rodents is the first finding report by Yoshizawa S and their colleagues in Fujiki's group [6]. They found that EGCG inhibited tumor promotion induced by teleocidin, a TPA type tumor promoter, in a two-

stage carcinogenesis experiment on mouse skin initiated with 7,12-dimethylbenz[a]anthracene (DMBA) as an initiator inhibited tumor promotion by teleocidin. EGCG also inhibited tumor promotion of okadaic acid on mouse skin initiated with DMBA. Okadaic acid is a potent inhibitor of protein phosphatases 1 and 2A (PP1 and PP2A). It is important to note that EGCG inhibits tumor promotion mediated through two different mechanisms: Activation of protein kinase C and inhibition of PP1 and PP2A [7]. After their finding, many scientists reported inhibitory effects of EGCG and GTE on tumor developments in various organs that induced by various chemical carcinogen in rodents, for example, digestive tract including esophagus, stomach, duodenum, colon and also liver, lung, pancreas, mammary gland, skin, bladder, and prostate [8]. Thus, EGCG and GTE have a wide range of target organs for their preventive effects. The study by administration of ^{3}H-EGCG into the mouse stomach revealed the wide distribution of ^{3}H-EGCG into the various organs, in which EGCG shows inhibitory effects of tumor development. Furthermore, duplicate administration of ^{3}H-EGCG enhances incorporation of ^{3}H-EGCG 4-6 times in blood, brain, lung, liver, pancreas, and bladder, indicating that drinking more green tea get the higher concentration of EGCG in the target organs [4,9]. Furthermore, 0.05% EGCG in drinking water inhibited metastasis of mouse melanoma cells into lung [10]. It is important to note that EGCG and GTE were not toxic for rodents. Thus, EGCG and GTE are effective cancer prevention in wide range of target organs in rodents.

1.1.3. Cancer preventive activity of green tea in human

Most Japanese drink green tea every day. Especially, people who live in the tea producing area, such as Saitama Prefecture, drink a lot of Sencha. The epidemiology

study in Saitama revealed cancer preventive activity in humans. The first finding cancer preventive activity of green tea in humans was reported by Imai K and Nakachi K [11]. The prospective cohort study with 8,552 individuals aged over 40 in Saitama Prefecture revealed that cancer onset for female patients who consumed more than 10 Japanese-size cups (equivalent to 2.5 g green tea extract) of green tea per day was delayed 7.3 years for females and 3.2 years for males compared with that for those who consumed less than 3 cups per day. It is important to note that the weaker preventive effects among males are partly due to higher tobacco consumption. This study also revealed that higher consumption of green tea most effectively reduced relative risk of lung cancer to 0.33, followed by liver (0.53), colon (0.56), and stomach (0.69) [12].

Green tea is effective for cancer prevention of primary cancer before cancer onset and prevention of recurrence of cancer after treatment. The case-control study at Saitama Cancer Center Hospital, Japan showed the preventive effect of recurrence of breast cancer. Among stages I and II of total 472 breast cancer patients, the group that consumed 8 cups of green tea per day showed a lower recurrence rate (16.7 %), and a longer disease-free period (3.6 years), than the group that consumed 3 cups per day (24.3 % of recurrence rate and 2.8 years of disease-free period) [13].

Cancer preventive activity of green tea was proved by phase II clinical trial. A double-blind randomized clinical phase II colorectal adenoma recurrence in patients who have no polyps after the polypectomy were conducted in Gifu University, Japan. And drinking 10 cups of green tea supplemented with GTE tablets reduced the recurrence of colorectal adenomas determined by the end-point colonoscopy [14]. The results showed that the recurrence rate of the control group (without GTE tablets) that maintained their usual daily consumption of green tea was 31 %, and that of the GTE tablets group that

drank at least 10 cups of green tea per day supplemented with GTE tablets was 15 %, a 51.6 % prevention [14]. These treatment used GTE tablet produced by the Saitama Prefectural Tea Research Institute that reduced the caffeine content from 5% to less than 3% [1]. A similar trial was conducted at Seoul National University, Korea by determined the preventive effect of GTE on metachronous colorectal adenomas. The subject who had complete removal of colorectal adenomas by endoscopic polypectomy were randomized into 2 groups: control group (without GTE supplementation) and supplementation group (with 0.9 g GTE per day for 1 year). The results showed that the incidence of metachronous colorectal adenomas were reduced 44.2 % at the end-point colonoscopy, by 42.3% in the control group and 23.6% in supplementation group. Moreover, the number of relapsed adenomas were also decreased in the supplementation group [15]. Furthermore, GTE showed the prevention effect of metachronous adenoma recurrence in Germany [16]. Moreover, treatment with green tea catechins showed the prevention of prostate cancer development in patients who had high-grade prostate intraepithelial neoplasia in Italy [17], as well as the prevention of oral premalignant leukoplakia in USA [18]. Therefore, green tea catechins are effective cancer preventive compounds in humans.

1.1.4. Synergistic enhancement of anti-cancer activity

Up to now, EGCG shows synergistic enhancement of anticancer activity in *in vitro* experiments by the combination of EGCG and 46 anticancer compounds in 58 human cancer cell lines via various mechanism pathways, and the synergistic inhibition of tumor volume of 13 combination experiments using xenograft mouse models in *in vivo* experiments [19]. Recently, our group have been reported the new finding of the combination of EGCG and a new synthetic retinoid Am80, a drug for treatment of acute

promyelocytic leukemia, showed strong induction of lung cancer cell apoptosis compared with Am80 alone or EGCG alone through down-regulation of histone deacetylases-4, -5, and -6. These combination changed the acetylation status in non-histone proteins and enhanced apoptosis via both $p21^{waf1}$ apoptotic pathway and growth arrest and DNA damage gene 153 (GADD153)-death receptor 5 (DR5) apoptotic pathway [20].

A treatment of head and neck cancer patients with erlotinib in the combination with GTE tablets are now going on in the USA [21]. Since there are many healthy cancer patients following treatment in Japan and around the world, therefore, the combination of green tea catechins and anticancer compounds is opening a new era in cancer therapeutic strategy [1,4,5,7,21,22].

1.1.5. Mechanisms of action of green tea catechins for anti-cancer activity

It is important to determine how a simple compound like EGCG or a mixture of green tea catechins induce numerous beneficial effects on cancer in humans, such as prevention of cancer development, inhibition of recurrence, and synergistic anticancer effect. Numerous studies indicate that EGCG and green tea catechins have multifunctional effects. Green tea catechins are a tannin and therefore have a high affinity with many biomolecules, including phospholipids, proteins, and nucleic acids [23].

As I aforementioned, EGCG inhibits two different pathways of tumor promotion: Activation of protein kinase C by TPA-type tumor promotion and inhibition of PP1 and PP2A by okadaic acid. Study of receptor binding using ^{3}H-TPA and ^{3}H-okadaic acid shows that TPA binds to the phorbol ester receptor, whereas okadaic acid binds to PP1 and PP2A on membrane fraction of mouse skin. The specific binding of ^{3}H-TPA and that of ^{3}H-okadaic acid showed decreasing immediately and reached a minimum

in 5 to 10 min after treatment with 5 mg EGCG on mouse skin. The results suggested that EGCG treatment inhibited the interaction of tumor promoters with their receptors resulting in inhibition of tumor promotion [7]. This is named "Sealing effect of EGCG." Furthermore, Yoshikawa's group evaluated the physical interactions of catechin derivatives–membrane interactions with the cell membrane model and found that green tea catechins with galloyl moiety are form aggregates in aqueous solutions and their adsorption onto the membrane surface resulting in stiffening of lipid membranes [24]. Atomic force microscope (AFM) is a physical biochemical tool used for cells stiffness (large elasticity) measurement [7,25,26]. AFM revealed that the low value of Young's moduli, indicating low cell stiffness, is associated with the high potential of cell migration and metastasis in various cancer cells. Gimzewski's group at The University of California, Los Angeles (UCLA) first found that treatment of metastatic tumor cells (obtained from the pleural effusion of patients with pancreas, lungs, ovary, and breast cancers) with GTE dramatically increased cell stiffness. However, GTE did not affect the cell stiffness of normal cell mesothelial cells in pleural effusions [7]. Since cell motility and cell stiffness are closely related to metastatic activity of cancer cells, Takahashi A et al. reported that EGCG inhibited molecular phenotypes of epithelial-mesenchymal transition (EMT), such as inhibition of cell motility and increase cell stiffness in highly metastatic human lung cancer cells, H1299 and Lu99 cells. EGCG showed inhibition of EMT phenotypes similar to methyl-β-cyclodextrin, a reagent to deplete cholesterol in the plasma membrane, suggesting that EGCG induces inhibition of EMT phenotypes by alteration of membrane organization resulting in cancer prevention [26]. Moreover, reflection interference contrast microscopy (RICM) is also used for measure the biophysical property of cancer cells. The self-assembled monolayer (SAM)-pattern

substrate and RICM visualizes the adhesion of cancer cells by physical contacts between a cell and substrate that optimized the diameter of a cell. The evaluation of time-lapse RICM revealed that highly metastatic mouse melanoma B16-F10 cells has slightly larger tight contact area than lowly metastatic B16-F1 cells. Treatment with EGCG decreased the tight contact area, resulting in that the reduction of adhesion in cancer cells treated with EGCG plays a mechanistic role in the inhibition of metastasis. So, the interaction of green tea catechin with lipid membrane alters adhesion of cancer cells [27].

The "sealing effects of EGCG" is prevention of the interaction of ligands with their receptors by covering the cell surface or competing ligands for binding to it receptors by EGCG (Figure 2) [28], and also the suppression of lipid raft-associated signaling proteins by lipid rafts disruption in the plasma membrane. Lipid rafts are dynamic of plasma membrane structures containing cholesterol and sphingolipids that regulate the cellular signaling mechanism by protein-protein interaction, receptor activation, and cellular signaling. And EGCG is able to modify and change the organization of lipid in the plasma membrane that causes the rearrangement of lipid rafts resulting in preventing the activation of cell surface receptors. The binding of a growth factor or a cytokine to the extracellular domain of receptor tyrosine kinases induces the dimerization and autophosphorylation on specific tyrosine residues and the activation of downstream intracellular signaling that includes Ras/extracellular-signal-regulated kinase (ERK)/ mitogen-activated protein kinases (MAPK) and phosphoinositide 3-kinase (PI3K)/AKT activation triggers a cascade of molecular events involving enzymes, proteins, and transcription factors. For example, EGCG inhibits the binding of epidermal growth factor (EGF) to the EGF receptor (EGFR) and the subsequent dimerization and activation of the EGFR by altering membrane organization [29]. Moreover, EGCG and green tea catechins

prevented by the interaction between receptor and ligand through membrane internalization [7]. EGFR is quickly internalized inside endosomal vesicles in human colon cancer cells treated with EGCG (1 μg/ml for 30 min). EGCG can induce internalization of EGFRs into endosomes, which can recycle back to the cell surface. The internalization makes the receptor inaccessible to EGF and abrogates receptor tyrosine kinases signaling cascade [30].

Therefore, EGCG and green tea catechins bring multi-mechanisms of action via the "sealing effects of EGCG" that interfere directly or indirectly with the formation of the ligand-receptor complex of several cell surface receptors, resulting in cancer prevention, inhibition of metastasis and synergistic activity with the combination (Figure 2).

1.1.6. PD-L1/PD-1 immune checkpoint

The immune checkpoint is a negative regulator of the immune activation for inhibition of T cell immune response to maintain normal immune homeostasis. It is a kind of co-stimulatory and the co-inhibitory signal of antigen and T cell receptor (TCR) recognition of immune response, resulting in promotes T-cell apoptosis, anergy, and exhaustion. Normally, antigen and T cell recognition requires 2 signals, first are TCR triggered by the major histocompatibility complex (MHC)-antigenic peptide complex, and the second signal is co-stimulation signal. It provides by co-stimulatory molecules expressed on the surface of antigen presenting cells (APC) and T cells, such as cytotoxic T-lymphocyte–associated antigen 4 (CTLA-4) and programmed cell death-ligand 1 (PD-1) molecules. Recently, PD-L1/PD-1 immune checkpoint pathway is an important mechanism utilized by tumors to escape antitumor response.

PD-1, a 50-55 kDa type I transmembrane protein, was discovered by Honjo T and his colleagues at Kyoto University [31]. The PD-1 (Pdcd1) gene is a CD28 family member that is a member of the immunoglobulin gene superfamily, locates on chromosome 2q.37.3. PD-1 is expressed on a variety of immune cells including T lymphocytes, B lymphocytes, natural killer (NK) T cells, activated monocytes, and dendritic cells. PD-1 is only expressed on the surface of activated T lymphocytes and not resting T cells. PD-1 is essential for the inhibitory function of TCR signaling [32,33]. PD-1 specifically binds to two known ligands, PD-L1 and PD-L2.

PD-L1 is also known as B7-H1 (CD274), is a mainly cell surface protein of B7 family member. PD-L1 is a 40 kDa type 1 transmembrane protein that encoded by the CD274 (Pdcd1-l1) gene and the full length of cDNA is 870 base pair [34]. Human PD-L1 gene is located on chromosome 9p24.1. PD-L1 is expressed on almost all types of lymphohematopoietic cells and APCs at varying levels and is constitutively expressed on T cells, B cells, macrophages and dendritic cells which involve in immune tolerance to prevent an autoimmune response. PD-L1 is abundant in various human cancer cells and finding appears to be important for cancer immunotherapy. The PD-L1 ligand is further upregulated and strongly induced by mitogenic stimulation and IFN-γ, which is activated of PD-1 receptor expression [35,36,37].

PD-L2 or PDCD1 ligand 2 is also known as butyrophilin B7-DC or CD273. It is a transmembrane protein encoded by programmed cell death 1 ligand 2 (PDCD1LG2) gene and is structurally similar to PD-L1. The PD-L2 gene is localized on human chromosome 9p24.1 same as PD-L1 gene. The PD-L2 expression is very limited in antigen-presenting cells, such as dendritic cells and macrophage. Induction of PD-L2 expression in other immune and non-immune cells by various microenvironmental

stimuli is lower than that of PD-L1 [35]. Although PD-L1 is the dominant ligand for PD-1, PD-L2 can bind to PD-L1 about 2- to 6-fold higher than that of PD-L1. However, the role of PD-L2 in mediating immunosuppression and in the human tumor microenvironment has not been clearly established [38].

1.1.7. Promotion of cancer immune escape by PD-L1 expression

Recent studies showed that tumor cells "edit" host immunity in several ways to evade immune defenses in the tumor microenvironment. This phenomenon is called "cancer immune escape." The tumor immune escape mechanisms are; Tumor has low immunogenicity; Tumor induces antigenic modulation; Tumor induces immune suppression; Tumor induces privileged site, and Tumor expresses "Don't eat me" signal on the cell surface or immune checkpoint. One of the most important molecular for immune escape is an immune checkpoint mediated by the PD-L1/PD-1 interaction. [39,40]. PD-L1 overexpression on tumor cells bind to PD-1 on activated T cells, leading to induce cancer to escape from the immune response by suppresses signal for regulating the antigen recognition of TCR, and then promotes T cell apoptosis, anergy and functional exhaustion (Figure 3) [41,42,43]. Therefore, blockade the PD-L1/PD-1 interaction is the potential basis for new cancer immunotherapy.

PD-L1 is varied levels expressed on the surface of various human cancers, including urothelial cancers [44], gastrointestinal cancers [45], breast cancer [46], melanoma [47], ovarian cancer [48,49], especially lung cancer [38,50,51,52] as well as on tumor-infiltrating immune cells in the tumor microenvironment [53]. PD-L1 is up-regulated by various proinflammatory cytokines, such as IFN-γ [54,55] and TNF-α [56,57] and growth factors [58] in the tumor microenvironment. The IFN-γ is the most

potential PD-L1 inducer secreted by infiltrating lymphocytes and tissue-recruiting immune cells under inflammatory conditions upon cancer. IFN-γ secreted from tumor-infiltrating CD8+ lymphocytes upregulates PD-L1 and promotes tumor progression in ovarian cancer cells [48]. PD-L1 is induced in tumor cells by exposure to hypoxia via the transcription factor hypoxia-inducible factor-1α (HIF-1α), leading to increased apoptosis of cytotoxic T lymphocytes [59]. Induction of PD-L1 expressions are involved by various signal pathways, such as nuclear factor κ-light-chain-enhancer of activated B cells (NF-κB), MAPKs, PI3K, mammalian target of rapamycin (mTOR), and Janus kinase/signal transducers and activators of transcription (JAK/STAT) mediated by the molecules triggers the nuclear translocation of various transcription factor [55]. Membrane expression of PD-L1 in NSCLC associated with PI3K/AKT-mTOR activation which plays a central role in the initiation of cytokines and growth factor stimulated gene translation [60]. Moreover, PD-L1 overexpression in subpopulation melanoma cells demonstrated that enhance tumorigenicity by modulates downstream effectors of mTOR signaling [61].

1.1.8. Immune checkpoint inhibitors

Immune checkpoint inhibitor is a type of immunotherapy using a monoclonal antibody. It blocks the interaction of immune checkpoint proteins and stops the immune system to attack the cancer cells. CTLA-4 antibodies were the first of immunotherapeutics to achieve US Food and Drug Administration (FDA) approval. The powerful CTLA-4 monoclonal antibodies are ipilimumab (Yervoy) and tremelimumab that have shown evidence of an anticancer effects to melanoma, lung, kidney, prostate, cervical, colorectal, gastric, pancreatic, ovarian and urothelial cancers. The immune checkpoint monoclonal

antibodies that block the activity of PD-1, Nivolumab (Opdivo) and pembrolizumab (Keytruda), are effective for treatment the cancer of lung, kidney, bladder, head and neck, liver, skin, colon, as well as relapsed or refractory classical Hodgkin's lymphoma. In particular, checkpoint inhibitors targeting PD-L1, atezolizumab (Tecentriq), avelumab (Bavencio) and durvalumab (Imfinzi), have demonstrated beneficial clinical activity in lung, bladder and Merkel cell skin cancers [43,62,63,64]. One of the inhibitors that succeed to cure advanced melanoma is Opdivo. Treatment melanoma with Opdivo, a PD-1 immune checkpoint inhibitor, increase the overall survival rate at 1 year by 73%, more effective than treatment with dacarbazine, an anti-cancer drug of melanoma, by 42% [65]. Moreover, treatment with Opdivo in patients with advanced NSCLC and high PD-L1 expression was associated with significantly longer progression-free and overall survival and with fewer adverse events compared with those with platinum-based chemotherapy [66,67].

1.2 Hypothesis and general objectives

To understand mechanism of the wide beneficial effects of EGCG to cancer preventives, I hypothesized that the "sealing effects of EGCG" could enhance the anti-tumor immunity via down-regulation of PD-L1 expression in lung cancer. Because the interaction of EGCG and lipid membrane reflects in stiffening of the cell membrane by alteration of membrane organization, it results in inhibition the interaction of various ligands to their receptors, probably including PD-L1 ligand. To investigate the functions of EGCG in anti-tumor immune response resulting in cancer prevention, I first examined the inhibitory effect of EGCG and green tea catechins on PD-L1 expression *in vitro* by using NSCLCs. Then, I examined the inhibition of PD-L1 expression in NNK-induced lung tumors in A/J mice by oral administration of GTE *in vivo* lung carcinogenesis experiment. Finally, I studied the effect of EGCG on restoring action of T cells activated by an *ex vivo* co-culture model experiment with tumor specific CD3+ T cells and F10-OVA cells, a model of tumor cells.

Chapter 2

Green tea catechins inhibit PD-L1 expression and lung tumor growth as an alternative immune checkpoint inhibitor

2.1. Introduction

In Japan, lung cancer is the leading cause of cancer deaths that caused by smoking [68]. Lung cancers, especially NSCLCs, are known well highly PD-L1 expression [38,69,70] which were induced by smoking [71]. Mutations of EGF receptor (EGFR), KRAS, and anaplastic lymphoma kinase (ALK) genes in NSCLC patients are also induced PD-L1 expression via activation of S6K/elF4B transcription factor [60,72,73]. The KRAS mutations up-regulates PD-L1 expression via AKT–mTOR, MEK or ERK signaling pathway [60,74,75]. The deletions exon-19 and L858R mutation in EGFR showed induction of PD-L1 expression through the p-ERK1/2/p-c-Jun pathway in NSCLC patients [76]. The PD-L1 expression is induced by smoking and a tobacco contains a variety of carcinogens, such as NNK, polycyclic aromatic hydrocarbons, nitrosamines, and aromatic amines. Among these carcinogens, NNK strongly induced PD-L1 expression in a mouse model of NSCLC driven by a mutation in KRAS or EGFR via AKT-mTOR pathway [60]. Moreover, NNK induces immune suppression in A/J mice; The NNK-induced lung adenomas/adenocarcinomas showed an increase in the number of tumors following the depletion of NK cells, suggesting that NNK might inhibit NK cells in lung cancer. NNK is also shown effect on cytotoxic T cells lymphocyte (CTL) activation by modulating adhesion molecule expression and reducing memory programming [77,78]. In tumor microenvironment, IFN-γ is the most potent stimulator of PD-L1 expression via IFN-γ receptor-associated Janus kinase (JAK) 1/JAK2/STAT

signaling cascade and activation of interferon regulatory factor (IRF) transcription factor in NSCLCs [48,79,80]. Among the members of the STAT family, STAT1 and STAT3 are the main PD-L1 gene up-regulators [81]. Therefore, NNK, EGF, and IFN-γ are important inducers of PD-L1 expression in NSCLCs.

PD-1 and its ligand PD-L1 are the most promising targets in immunotherapies for NSCLC. The interaction between PD-1 and PD-L1 inhibits the proliferation and activation of T cells, leading to the immune escape of tumor cells. Blocking the PD-L1/PD-1 pathway can enhance the antitumor immunity by restoring the action of T cells, such as CTLs activity and IL-2 production [82,83,84,85]. It is important to note that IL-2 is strictly required in the process of CTL induction and its survival. While PD-1 inhibitors, nivolumab, and pembrolizumab, have been approved for treatment of NSCLC, atezolizumab is the first PD-L1 inhibitor to receive FDA approval for metastatic NSCLC patients who have progressed on frontline chemotherapy [86]. However, treatment of cancers with PD-L1/PD-1 inhibitors is high costs and can lead to immune-related adverse events, which could be serious and even fetal [87]. Therefore, small molecule inhibitors of PD-L1 expression other than the monoclonal antibodies are possible promising and effective cancer preventives. Recently, bromodomain and extraterminal (BET) protein inhibitors were reported as PD-L1 inhibitors by directly binding to BRD4, which regulate PD-L1 gene, resulting in the inhibition of PD-L1 expression at the transcription level. And inhibition of BRD4 suppresses PD-L1 expression and increases CTL activity to limit tumor progression *in vivo* in ovarian cancer models [88]. Apigenin, a flavonoid class of phytochemicals, is also a PD-L1 inhibitor to enhance T cell proliferation and anti-tumor immune response in breast cancer [85]. The combination of *Strongylocentrotus nudus* egg polysaccharide (SEP), a D-glucan containing an α-1,4-linked backbone and α-1,6-linked

branches from *Strongylocentrotus nudus* eggs (Sea urchins, known as Uni in Japanese), with PD-L1 monoclonal antibodies had potent activity in promoting T cells proliferation and cytokines secretion including IL-2 and IFN-γ by activating MEK/ERK pathway in melanoma [89]. Thus, development of small-molecules blocking PD-1/PD-L1 signaling is actively being investigated.

Recently, human cancer stem cells (CSCs) are a target for cancer prevention using EGCG, and that EGCG inhibits the self-renewal of CSCs and the expression of epithelial-mesenchymal transition (EMT) phenotypes by alteration of membrane organization, such as stiffening of the cell membrane [5,26,90]. Although various biochemical and molecular biological effects with green tea catechins have been reported, their effects on anti-tumor immunity were not well known. NNK induced PD-L1 protein in lung tumors [60] and oral administration of GTE inhibited NNK-induced lung tumor development in A/J mice [91]. Furthermore, the prospective cohort study revealed that lung cancer is the most effective target organ in humans [11]. Based on these results, I think EGCG might bring additional clinical benefits through immunological interactions, PD-L1/PD-1 pathway, based on the "sealing effects of EGCG" which green tea catechin has the capacity to bind to various proteins and nucleic acids [7,92].

To clarify the effect of GTE and green tea catechins on PD-L1 expression in NSCLCs, I established an *in vitro* experiments of IFN-γ- and EGF-induced PD-L1 expression. This is because IFN-γ is the strongest stimulator of PD-L1 expression, and EGF and EGF-receptor (EGFR) mutations induce PD-L1 expression with lung cancer progression [93,94,95]. I then examined whether EGCG inhibited PD-L1 expression induced by IFN-γ or EGF along with an investigation of the mechanisms on signaling pathway. I found that EGCG inhibited PD-L1 expression by blocking the IFN-γ-induced

JAK2/STAT1 signaling pathway and EGF-induced EGFR/AKT signaling pathway. I next examined whether oral administration of GTE reduced PD-L1 expression in NNK-induced lung tumors in A/J mice, *in vivo*, by immunohistochemistry with a specific PD-L1 antibody. And I found that oral administration of GTE showed a reduction in the average number of tumors per mouse and the percentage of PD-L1 positive cells in the lung tumors in A/J mice treated with NNK. I next clarify whether EGCG restores anti-tumor immune escape mediated through enhanced T cells activity and IL-2 expression, an indicator of activated T cells. I conducted a co-culture experiment with mouse melanoma ovalbumin-expressing B16-F10 (F10-OVA) cells and tumor-specific CD3+ T cells isolated from the spleen of F10-OVA-immunized C57BL/6, an *ex vivo* model that determine the induction of effective T cells [96]. I found that pretreatment with EGCG restored T-cells activity by reduced PD-L1 mRNA level in F10-OVA cells, and increased IL-2 mRNA expression in T cells and also enhanced apoptosis of F10-OVA cells. This is the first report that EGCG and GTE act as immune checkpoint inhibitors for lung cancer development.

2.2. Materials and Methods

2.2.1. Cell lines and reagents

NSCLCs cell lines A549, H322, H1703, and H1299 were obtained from the American Type Culture Collection, RERF-LC-AI (LC-AI) and Lu99 cell lines were from Riken Bioresource Center (Ibaraki, Japan). Mouse B16-F10 melanoma was kindly provided by Dr. Shun'ichiro Taniguchi at Shinshu University, Japan. Cells were cultured in Roswell Park Memorial Institute (RPMI) 1640, Minimum Essential Medium (MEM) (for LC-AI) (Nissui, Tokyo, Japan) or Dulbecco's Modified Eagle Medium (DMEM) (Nissui, Tokyo, Japan) medium containing 10% heat-inactivated fetal bovine serum (FBS) (Nichirei Biosicence Inc., Tokyo, Japan), 5.7 units/ml of penicillin and streptomycin (Gibco Brl, CA, USA), 1 mM L-glutamine (Sigma Aldrich, STL, USA), and 23.8 mM sodium bicarbonate (Gibco Brl, CA, USA). The cells were maintained at 37°C and 95% relative humidity with 5% CO_2 level. EGCG (more than 99% purity) was purified from Japanese green tea leaves, and GTE was extracted by a similar procedure to make green tea infusion (Sencha) as described previously [22]. Green tea leaves were cultivated at Saitama Prefectural Tea Institute, Saitama, Japan, and processed to make Sencha. After brewing 2 kg of green tea leaves (Sencha) in 70 L of hot water (85°C) for 15 min, the green tea infusion was filtrated and freeze-dried. About 500 g GTE was obtained. This GTE contained 14% EGCG, 8% ECG, 3% EGC, and 3.5% EC and 3.3% caffeine as analyzed by HPLC. ECG (>99%), EGC (>99%) and EC (>99%) were purchased from Funakoshi Co. Ltd., Tokyo, Japan.

Reagents used are as follows:

Reagents	Company
Recombinant human IFN-γ	R & D Systems, MN, USA
Recombinant mouse IFN-γ	R & D Systems, MN, USA
Recombinant human EGF	Peprotech, London, UK
Recombinant human TNF-α	R & D Systems, MN, USA
Recombinant mouse Interleukin-2 (IL-2)	Cell Signaling Technology, MA, USA
Fludarabine	Selleck Chem, TX, USA
G418 sulfate	Calbiochem, CA, USA
MEM non-essential amino acids	Gibco Brl, CA, USA
Mitomycin C	Cell Signaling Technology, MA, USA
SB-203580	EMD Millipore, MA, USA
Sodium pyruvate	Gibco Brl, CA, USA
TG-101348	Funakoshi, Co. Ltd., Tokyo, Japan
UO-126	Funakoshi, Co. Ltd., Tokyo, Japan
Wortmannin	Sigma Aldrich Technology, MO, USA

All antibodies used are as follows:

Antibodies	Company	Dilution	Anti-IgG
Human PD-L1	Abcam, MA, USA	1:1000 in 3% skim milk	Rabbit
STAT1	BD Bioscience, NJ, UK	1:1000 in 5% BSA	Mouse
Phospho-STAT1	BD Bioscience, NJ, UK	1:1000 in 5% BSA	Mouse
STAT3	BD Bioscience, NJ, UK	1:2500 in 5% BSA	Mouse
Phospho-STAT3	BD Bioscience, NJ, UK	1:500 in 5% BSA	Mouse
p44/42 MAPK	Cell Signaling Technology, MA, USA	1:1000 in 5% BSA	Rabbit
Phospho-p44/42 MAPK	Cell Signaling Technology, MA, USA	1:1000 in 5% BSA	Rabbit
Akt	Cell Signaling Technology, MA, USA	1:1000 in 5% BSA	Rabbit
Phospho-Akt	Cell Signaling Technology, MA, USA	1:1000 in 5% BSA	Rabbit
p-38 MAPK	Cell Signaling Technology, MA, USA	1:1000 in 5% BSA	Rabbit
Phospho-p-38 MAPK	Cell Signaling Technology, MA, USA	1:1000 in 5% BSA	Rabbit
IκB-α	Santa Cruz Biotechnology, CA, USA	1:200 in 5% BSA	Rabbit
GAPDH	Trevigen, MD, USA	1:4000 in 3% skim milk	Rabbit

Anti-IgG horseradish peroxidase (HRP) conjugated antibody is were used as a secondary of western blotting as follows:

Antibodies	**Company**	**Dilution**
Anti-rabbit IgG	GE Healthcare, Hertfordshire, UK	1:2000 in 3% skim milk
Anti-mouse IgG	Santa Cruz, CA, USA	1:2000 in 3% skim milk

2.2.2. Treatment with green tea catechins and IFN-γ or EGF

NSCLCs 5 x 10^5 cells/3.5 ml appropriate medium containing 1% FBS were seeded into 6 cm dish and then incubated for overnight. EGCG or other green tea catechins (ECG, EGC, and EC) at 25 mM were dissolved in 20% ethanol in phosphate buffered saline (PBS). Freshly prepared catechins were diluted with appropriate medium, and then 500 μl solution was added to the cells. Three hours after incubation, IFN-γ or EGF were added.

2.2.3. RNA extraction and quantitative real-time RT-PCR (qRT-PCR)

Total RNA of NSCLC cell lines were extracted with ISOGEN (Nippon Gene Co. Ltd., Tokyo, Japan). Complementary DNA (cDNA) was synthesized from total RNA using $Oligo(dT)_{16}$ and MuLV reverse transcriptase (Thermo Fisher Scientific, MA, USA). Gene expression was quantified using SYBR Green I (LightCycler 480, Roche Lifescience, Basel, Switzerland) using specific primers as follows:

Primer name		5'- nucleotide sequence-3'
Human PD-L1	Forward	GGACAAGCAGTGACCATCAAG
	Reverse	CCCAGAATTTACCAAAGTGAGTCCT
Human PD-L2	Forward	ATTGCAGCTTCACCAGATAGC
	Reverse	AAAGTTGCATTCCAGGGTCAC
Mouse PD-L1	Forward	GCTCCAAAGGACTTGTACGTG
	Reverse	TGATCTGAAGGGCAGCATTTC
Mouse PD-1	Forward	CCAAGGCGCAGATCAAAGAGA
	Reverse	AGGACCCAGACTAGCAGCA
Mouse IL-2	Forward	TTGTCGTCCTTGTCAACAGC
	Reverse	CTGGGGAGTTTCAGGTTCCT
Human GAPDH	Forward	TGGTATCGTGGAAGGACTCATGAC
	Reverse	ATGCCACTCAGCTTCCCGTTCAGC
Mouse GAPDH	Forward	TGGCATTGTGGAAGGGCTCATGAC
	Reverse	ATGCCAGTGAGCTTCCCGTTCCAGC
Ovalbumin	Forward	AGAAATGTCCTTCAGCCAAGCTC
	Reverse	GCCCATAGCCATTAAGACAGATGTG

The PCR program used: 95°C for 5 min, then 45 cycles: 95°C for 15 sec, melting temperature (Tm) 60°C for 5 sec, 72°C for 10 sec. Relative PD-L1 mRNA expression was normalized by GAPDH mRNA expression as an internal control. Results were obtained from at least 3 independent experiments.

2.2.4. Western blotting

After treatment with IFN-γ or EGF with or without green tea catechins, cells were washed with ice-cold PBS. Whole cell lysates are obtained by radioimmunoprecipitation assay (RIPA) buffer containing 50 mM Tris-HCl (pH 7.4), 1% NP-40, 0.5% sodium deoxycholate, 0.1% sodium dodecyl sulfate (SDS), 150 mM sodium choline, 2mM ethylenediaminetetraacetic acid (EDTA), 10 μg/ml aprotinin, 10 μg/ml leupeptin, 1 mM phenylmethanesulfonyl fluoride, 2.5 mM sodium pyrophosphate, 1 mM sodium orthovanadate and 2.5 mM sodium fluoride. Then, cell lysate was sonicated for 5 min on ice and centrifuged at 12,000 rpm at 4°C. The supernatant was used as the whole cell lysate. The cell lysate proteins were kept at -20°C. Protein concentration was determined using bovine serum albumin (BSA) by Bradford protein assay. The lysate was dissolved in SDS-sample buffer and denatured by boiling at 92°C for 5 min, and stored at -20°C.

Lysates were applied onto 8, 10 or 12% (depended on the molecular weight of the target protein) SDS-polyacrylamide gel and separated by electrophoresis (SDS-PAGE), then transferred onto nitrocellulose membranes. The membranes were incubated with 3% skim milk in 20 mM Tris-HCl (pH 7.6) and 150 mM NaCl with 0.1% Tween 20 (TBS-T) for 2 h, then incubated with appropriate primary antibody overnight at 8°C. After washing with TBS-T 3 times, a membrane was incubated with HRP-secondary antibody against rabbit IgG or mouse IgG, the bound antibody was detected with Immunostar LD (Wako Pure Chemical Industries, Ltd., Osaka, Japan) using C-DiGit Chemiluminescent Western Blot Scanner (LI-COR Biosciences Inc., NE, USA). GAPDH protein expression was used as an internal control. The values are the average fold changes for non-treated cells obtained from at least 3 independent experiments.

2.2.5. Flow cytometry

After treatment with IFN-γ or EGF with or without green tea catechins, A549, H1299 and Lu99 cells (5 x 10^5 cells) were harvested by trypsinization and followed by centrifugation at 3,000 rpm at 4°C for 3 min. Suspended cells were stained with the anti-PD-L1 antibody (1:200) in 100µl of PBS containing 2% FBS and 0.02% EDTA for 30 min, on ice. After washing with 500 µl PBS, cell were centrifuged at 2,000 rpm at 4°C for 2 min, and then cells were suspended with Alexa Fluor 488 goat anti-rabbit IgG [H+L] (Invitrogen, CA, USA) (1:200) in 100µl of PBS containing 2% FBS and 0.02% EDTA for 20 min on ice in dark. After washing, cell pellets were suspended with 500 µl PBS and filtrated by Corning™ Falcon™ polystyrene round-bottom tube with cell strainer snap cap (Stemcell Technologies, Vancouver, Canada). Finally, cells were analyzed by using FACS flow cytometry (FACSCanto II, BD Biosciences, NJ, USA). The data were analyzed by the Flowjo ver.10 software (FlowLo, LLC, OR, USA). The cell-surface PD-L1 levels were determined by subtracting the Median Fluorescence Intensity (MFI) of control (cells stained with a secondary antibody without the first antibody). The experiments were performed at least three times, and data were expressed mean ± standard deviation (SD).

2.2.6. NNK-induced lung carcinogenesis experiment in A/J mice

The animal experiments were performed in accordance with a protocol approved by the Institutional Animal Care and Use Committee of the Research Institute for Clinical Oncology, Saitama Cancer Center. Seven-week-old female A/J mice (Japan SLC Inc., Shizuoka, Japan) were given a single intraperitoneal (i.p.) injection of NNK (100 mg/kg body weight, Toronto Research Chemicals Inc., Ontario, Canada). Two days later, 15

mice received drinking water containing 0.3% GTE and 20 mice received untreated drinking water. Mice continued to receive the indicated drinking water for 16 weeks [97,98]. GTE solution was prepared twice per week. After 16 weeks, lungs were kept in 10% buffered formalin solution. Lung tumors measuring 0.8 mm or more in diameter were counted.

2.2.7. Immunohistochemical staining

Lung tissue sections in paraffin block were deparaffinized and rehydrated through xylene and serial dilutions of ethanol and distilled water. They were then incubated with 3% H_2O_2 for 10 min to block endogenous peroxidase activity. The sections were subjected to antigen retrieval using pressure cooking in antigen activating solution (pH 9.0, 98°C) for 45 min and followed by slow cooling for 20 min. The sections were incubated with Protein Block (Dako, CA, USA) at room temperature for 5 min before incubation with anti-PD-L1 antibody at 37°C for 40 min. The secondary antibody (N-Histofine Simple Stain MAX-PO (Multi), Nichirei Bioscience Inc., Tokyo, Japan) was treated at 37°C for 20 min, and followed by staining with 3, 3'-diaminobenzine tetrahydrochloride as a chromogen and Mayer's hematoxylin as a counterstain (DAKO Liquid DAB+, Agilent Pathology Solutions, Dako, CA, USA), as described previously [99]. PD-L1 protein presented in a plasma membrane were counted as positive cells individually by three investigators. The percentage of positive cells were calculated with total cells as below. Results were expressed as average percentage of PD-L1 positive cells ± standard error (SE).

$$\% \text{ of PD-L1 positive cells} = \frac{\text{PD-L1 positive cells}}{\text{Total number of cells}} \times 100$$

2.2.8. Establishment of ovalbumin-expressing B16-F10 (F10-OVA) cells

F10-OVA cells that expressing ovalbumin were established by transfection of pcDNA3-OVA plasmid (Addgene, MA, USA) using Lipofectamine® 3000 Transfection Reagent (Invitrogen, Thermo Fisher Scientific, CA, USA) to B16-F10 cells. F10-OVA cells were maintained with 2 mg/ml G418 sulfate in DMEM containing 10% FBS. The F10-OVA clones were confirmed by *ovalbumin* gene expression using PCR.

2.2.9. Isolation of tumor specific CD3+ T cells

The animal experiments were performed in accordance with a protocol approved by the Institutional Animal Care and Use Committee of Saitama University. All efforts were made to minimize animal suffering and to reduce the number of animals used in the experiments. Female C57BL/6 mice (Japan SLC Inc., Shizuoka, Japan) at 6-8 weeks-old were used for isolation of tumor specific CD3+ T cells by immunization of mice with F10-OVA.

F10-OVA (1×10^7) cells/ml were treated with 25 μg/ml of mitomycin C in DMEM containing 10% FBS, then incubated for 20 min at 37°C, in dark. And then cells were washed with 10 ml DMEM medium for 3 times and centrifuged at 1,000 rpm for 3 min. Mitomycin C-treated F10-OVA (5×10^6) cells were suspended in 100 μl saline (0.9% of sodium chloride), and i.p. injected into the female C57BL/6 mouse. Fourteen days later, three mice were euthanized by i.p. injection with 300 μl of 26% sodium pentobarbital and their spleens were kept in RPMI medium containing 10% FBS on ice. Making a single cell by cut and mince using glass slides, and then passed through the cells as gently by using needle No. 18G, 24G, and 27G, sequentially. After that, the cells suspension were

filtrated by using Fisherbrand™ sterile cell strainers 40 μm (Fisher Scientific, NH, USA). The cells were collected after centrifugation at 1,000 rpm for 10 min. The cells were suspended with 20 ml red blood cell lysis buffer (Quicklysis™, Cytognos SL, Salamanca, Spain), and then incubated for 10 min at room temperature in dark. The reaction was stopped by the addition of 30 ml PBS and count the total number of T cells by the trypan blue exclusion method.

Next, the tumor specific CD3+ T cells were isolated from the splenic T lymphocytes using CD3+ MicroBead kit with MS column miniMACS^{TM} separator (Miltenyi Biotec GmbH, Bergisch Gladbach, Germany), according to the manufacturer's instructions. Fresh tumor specific CD3+ T cells were maintained in sensitization medium; Iscove's Modified Dulbecco's medium (IMDM) containing 1 mM sodium pyruvate and x1 nonessential amino acids, in the presence of 30 units/ml IL-2 and 10% FBS (Lot No. AHJ9164, HyClone road Logan, Utah, USA).

2.2.10. Cytotoxic assay with tumor specific CD3+ T cells

For cytotoxicity assay, tumor specific CD3+ T cells were used as effector and F10-OVA cells were used as targets. Mitomycin C-treated F10-OVA cells (2 x 10^5) in DMEM containing 1% FBS were seeded in 6 cm dish, and then changed to IMDM medium containing 10% FBS, 1 mM sodium pyruvate, x1 nonessential amino acids and 30 units/ml IL-2. After F10-OVA cells were treated with EGCG at various concentrations for 3 hrs, CD3+ T cells (2 x 10^6 cells) were added to F10-OVA cells and incubated for 48 h at 37 °C. The ratio of target cells (F10-OVA) and effector cells (CD3+ T cells) was 1:20. After co-culture in the absence or presence of EGCG for 48 h, T cells were collected and counted by Trypan blue exclusion method. Then, all T cells were kept in ISOGEN

solution for mRNA extraction. Co-cultured F10-OVA cells were harvested by trypsinization for apoptosis analysis and also kept in ISOGEN solution for mRNA extraction.

2.2.11. Analysis of apoptosis

Apoptosis was examined by flow cytometry of propidium iodide (PI)-stained cells. After co-cultured with tumor specific CD3+ T cells, trypsinized F10-OVA cells were fixed in ice-cold 70% ethanol, then treated with 50 μg/ml PI (Sigma-Aldrich Technology, MO, USA) for 30 min at room temperature. After filtration by strainer snap cap (Stemcell Technologies, Vancouver, Canada), PI-stained cells were analyzed using a FACS Flow cytometer (FACSCanto II, BD Biosciences, NJ, USA), as described previously [20]. Percentages of sub-G1 phase cells corresponding to apoptotic cells were analyzed by using FlowJo ver.10 (FlowJo, LLC, OR, USA).

2.2.12. Statistical analysis

Statistical analyses for differences of experiments were evaluated by one-way ANOVA followed by Dunnett's Multiple Comparisons Test, and that for the *in vivo* lung carcinogenesis experiments were conducted using non-parametric analysis with Wilcoxon-Mann-Whitney or Student's *t*-test. The p-value < 0.05 was considered to be statistically significant. Independent experiments were conducted at least 3 times, and values are expressed as the mean ± SD or ± SE (for animal experiments). Statistical analyses were performed using KaleidaGraph Ver. 4.1J (Synergy Software, Reading, PA, USA).

2.3. Results

2.3.1. Green tea catechins inhibited PD-L1 expression and lung tumor development

2.3.1.1. Intrinsic PD-L1 expression levels varied among NSCLCs

I examined the basal level of PD-L1 mRNA expression by qRT-PCR and total PD-L1 protein by western blotting in six human NSCLC cell lines; two adenocarcinomas (A549 and H322), two squamous cell carcinomas (H1703 and LC-AI) and two large cell carcinomas (H1299 and Lu99), and found that Lu99, LC-AI, and A549 cells show higher PD-L1 mRNA expression than that H322, H1299 and H1703 cell lines did (Figure 4A). And PD-L1 protein levels were similar to mRNA expression (Figure 4B). However, A549 cells showed low PD-L1 protein although PD-L1 mRNA levels were high. I classified these cell lines as follows: LC-AI and Lu99 cell lines showed the highest PD-L1 expression. A549 and H322 cell lines were medium, and H1703 and H1299 were very low. Three representative cell lines, Lu99 for high PD-L1 expression, A549 for medium, and H1299 for low expression were used for the further experiments. Their cell-surface PD-L1 levels were confirmed protein levels by flow cytometry (Figure 4C). The average MFI values of Lu99, A549, and H1299 cells show 3998.7, 1200.0, and 484.7, respectively. These results demonstrated that intrinsic PD-L1 expression levels were depended on its mRNA levels.

2.3.1.2. IFN-γ and EGF induced PD-L1 mRNA and protein in three NSCLC cell lines

Since it is well known that IFN-γ, produced by activated T cells, stimulates PD-L1 expression in tumor microenvironment [93,94], and activation of EGFR signaling by EGF and EGFR mutations also drove PD-L1 expression in NSCLC cells [60,95], so I

chose IFN-γ and EGF as PD-L1 inducer. Both IFN-γ and EGF increase PD-L1 protein expression through activation of mTOR signaling in NSCLC cells [60]. I found IFN-γ and EGF rapidly induced the expression of PD-L1 mRNA at an early time point, 3 h after treatment with IFN-γ in A549 and H1299 as well as treatment with EGF in Lu99 cells. PD-L1 mRNA level was decreased after 10 h treatment and kept until 48 h (Figure 5).

PD-L1 mRNA expression after in three cell lines was examined treatment with IFN-γ or EGF for 24 h. Treatment with 10 and 20 ng/ml IFN-γ significantly increased PD-L1 mRNA expression about 3-fold in A549, 6-fold in H1299 and 3-fold in Lu99 cells. On the other hand, treatment with 5 and 10 ng/ml EGF increased PD-L1 mRNA expression about 2.5-fold in A549 and 3-fold in Lu99 cells but did not in H1299 cells (Figure 6A). Total PD-L1 proteins were also increased by treatment with 20 ng/ml IFN-γ, 2-fold in A549 cells and 2.8-fold in H1299 cells, and slightly increased in Lu99 cells. On the other hand, treatment with 5 ng/ml EGF increased 2.4-fold in Lu99 cells and slightly increased in A549 cells, but did not change in H1299 cells (Figure 6B).

Cell-surface PD-L1 levels examined by flow cytometry analysis showed IFN-γ dose-dependently stimulated cell-surface PD-L1 expression in A549 and H1299, but not Lu99 cells (Figure 6C). And EGF stimulated cell-surface PD-L1 only Lu99 cells (Figure 6D). Therefore, I chose IFN-γ for A549 and H1299 cells and EGF treatment for Lu99 cells, and the 10 ng/ml of IFN-γ and EGR to increase cell-surface PD-L1 about 2.5-fold, for examination of the inhibitory effect of green tea catechins.

When I examined IFN-γ receptor 1 (IFNGR1) and IFNGR2 mRNA level and EGFR mRNA and protein levels in three cell lines, I found that IFNGR1 and IFNGR2 mRNA are similarly expressed among three cell lines (Figure 7A), but EGFR mRNA and protein were different. H1299 cells showed the lowest EGFR mRNA and protein levels

followed by A549 cells (3-fold) and Lu99 cells (10-fold), respectively (Figure 7B and 7C).

2.3.1.3. Green tea catechins and GTE reduced IFN-γ-induced cell-surface PD-L1 in A549 cells

Frist, I examined whether pretreatment with GTE and four catechins (EGCG, ECG, EGC, and EC) inhibit IFN-γ-induced cell-surface PD-L1 expression in A549 cells. I found GTE significantly reduced cell-surface PD-L1 in a dose-dependent manner. GTE 100 μg/ml strongly reduced cell-surface PD-L1 about 50%, and 50 μM EGCG, ECG, and EGC reduced cell-surface PD-L1 about 40-60%, but EC, an inactive catechin, did not (Figure 8). It is important to note that pretreatment with GTE and green tea catechins does not affect the viability of A549 cells. These results demonstrated that GTE, which contains several catechins, show strong inhibition IFN-γ-induced-cell-surface PD-L1 expression.

2.3.1.4. EGCG inhibited IFN-γ-induced PD-L1 mRNA and protein in A549 and H1299 cells

To further understand the inhibitory mechanism of PD-L1 expression with green tea catechins, I examined the effect of EGCG on IFN-γ-induced PD-L1 expression at mRNA, protein and cell-surface level. As shown in Figure 9, pretreatment with EGCG dose-dependently reduced mRNA, total protein and cell-surface PD-L1 levels: 10 and 50 μM EGCG showed 14 and 86% in mRNA level (Figure 9A), 57 and 80 % inhibition in protein level (Figure 9B), and 51 and 68% inhibition in cell-surface PD-L1 level (Fig. 9C). Similarly, EGCG showed inhibition of PD-L1 expression in H1299 cells. PD-L1

expressions were increased 26.3-fold on mRNA by treatment with IFN-γ, 5.4-fold for total protein and, 2.9-fold for cell-surface PD-L1 in H1299 cells (Figure 10). Pretreatment with EGCG reduced mRNA levels along with protein and cell-surface PD-L1 levels in a dose-dependent manner: 10 and 50 μM EGCG showed 63 and 86% inhibition in mRNA level (Figure 10A), 65 and 67 % inhibition in protein level (Figure 10B), and 45 and 54% inhibition in surface PD-L1 level (Figure 10C). These results clearly indicate that EGCG inhibited IFN-γ induced PD-L1 expression at the transcriptional levels.

2.3.1.5. EGCG inhibited IFN-γ-induced phosphorylation of STAT1 compared with STAT1- and JAK2-inhibitors

To understand how EGCG inhibit PD-L1 mRNA expression induced by IFN-γ, I first studied the IFN-γ receptor signaling pathway examined by the phosphorylation of signaling proteins, including STAT1, STAT3, AKT, MAPK and protein levels of IκB-α protein level. After treatment A549 and H1299 cells with IFN-γ for 30 min, I found IFN-γ strongly induced phosphorylation of STAT1 at tyrosine 701 (Tyr701), and slightly increased phosphorylation of AKT at serine 473 (Ser473), whereas IFN-γ did not affect phosphorylation of STAT3 and p42/44 MAPK, or IκB-α protein (Figure 11). The results indicate that IFN-γ-induced phosphorylation of STAT1 and AKT.

Pretreatment with EGCG dose-dependently inhibited IFN-γ-induced phosphorylation of STAT1 in both A549 and H1299 cells: Fifty μM EGCG showed 85% inhibition in A549 cells (Figure 12A), and 60% inhibition in H1299 cells 60% (Figure 12B), but wortmannin, a PI3K inhibitor, did not. Next, I confirm this using fludarabine, SB203580, UO126, and TG-101348. These results indicate that EGCG inhibits IFN-γ-induced PD-L1 expression via STAT1 signaling. Ten μM EGCG inhibited IFN-γ-induced

PD-L1 stronger than 10 μM fludarabine did (about 60%), and also EGCG was stronger effect than SB203580 and UO126 inhibitor (Figure 13A and B). Furthermore, pretreatment of A549 cells with 1 μM TG-101348, a JAK2 inhibitor, reduced IFN-γ-induced phosphorylation of STAT1 about 93% reduction (Figure 14A). Also, 1μM TG-101348 showed reduced cell-surface PD-L1 level about 60% reduction, in a similar manner to 50 μM EGCG (Figure 14B), but wortmannin did not. Thus, I conclude that EGCG inhibited PD-L1 expression via IFNR-JAK2-STAT1 axis.

2.3.1.6. EGCG inhibited EGF-induced PD-L1 mRNA and protein in Lu99 cells via AKT signal pathway

Lu99 cells constitutively express the cell-surface PD-L1 protein, and treatment of 10 ng/ml EGF significantly increased mRNA, total protein and cell-surface PD-L1 level about 3-fold, as shown in Chapter 2.3.1.2. Pretreatment with 50 μM EGCG for 3 h significantly inhibited levels of PD-L1 mRNA and protein by 50% and 37%, respectively (Figure 15A and 15B), and EGCG slightly inhibited cell-surface PD-L1 level to 2.3-fold (20% reduction) from 2.7-fold (Figure 15C). Treatment of Lu99 cells with EGF increased phosphorylated AKT about 3-fold, but not p-STAT1, p-STAT3 or p-p42/44 MAPK, and IκB-α protein was not affected (Figure 16) in Lu99 cells. Pretreatment with 50 μM EGCG reduced p-AKT by 35% and 1 μM wortmannin completely reduced the phosphorylation of AKT (Figure 17). Although the effects of EGCG on the EGFR/AKT axis were not strong, EGCG was able to inhibit the production of EGF-induced PD-L1 via AKT axis.

2.3.1.7. EGCG inhibited PD-L2 mRNA expression induced by IFN-γ or EGF

Although PD-L1 is the predominant of ligand PD-1, PD-L2 is also acting as a

ligand for PD-1 [35]. I found that treatment with IFN-γ increased PD-L2 mRNA expression in A549 and H1299 cells. So, I examined the effect of EGCG on PD-L2 expression. Pretreatment with 50 μM EGCG showed 77% and 88% reduction of PD-L2 mRNA level in A549 (Figure 18A) and H1299 (Figure 18B), respectively. In contrast, EGF did not induce PD-L2 mRNA expression in Lu99 cells (Figure 18C).

2.3.1.8 Oral administration of GTE inhibited lung tumor development induced by NNK and reduced PD-L1 positive cells in the tumors

To clarify the relationship between inhibition of PD-L1 expression and lung cancer prevention with green tea catechins *in vivo*, I conducted lung carcinogenesis experiment with NNK, a tobacco-specific carcinogen, in A/J mice. Experimental groups have consisted of two groups: NNK and NNK + GTE groups. In the NNK group, 20 mice were injected NNK (100 mg/kg body weight) intraperitoneally and given water for 16 weeks. And in NNK + GTE group, 15 mice were given 0.3% GTE in a drinking water 2 day after NNK injection. Lung tumors were developed in all mice of both groups. The number of tumors larger than 0.8 mm in a diameter were counted. I found that oral administration of GTE reduced average numbers of tumors per mouse from 4.1 ± 0.5 to 2.6 ± 0.4, a decrease of 37%. GTE clearly inhibited lung tumor development by NNK.

Immunohistochemical staining with specific anti-PD-L1 antibody revealed that PD-L1 protein presented on the plasma membrane and in the cytosol in lung tumor cells in both groups (Figure 19A). Numbers of cells expressing PD-L1 protein on the plasma membrane were counted as PD-L1 positive cells (Figure 19A and 19B). The NNK group had an average 9.6 ± 4.9% PD-L1 positive cells (0.2 % ~ 17.8%), while NNK + GTE group had 2.9 ± 2.2% (0% ~ 7.3%), a decrease of 70% (Figure 19 B and 19C). That is,

GTE significantly reduced PD-L1 protein in lung tumors *in vivo*, correlating well with inhibition of tumor development.

It is important to note that 0.3% (3 g/L) GTE containing 0.85 g/L catechins (14% EGCG, 8% ECG, 3% EGC and 3.5% EC) and 0.1 g/L caffeine, and is same as green tea beverage which Japanese drink every day. This is the first finding that oral administration of GTE significantly reduced % of PD-L1 positive cells, probably leading to lung cancer prevention.

2.3.2. EGCG stimulated the anti-tumor response of T cells by inhibition of PD-L1 expression

2.3.2.1. EGCG inhibited IFN-γ-induced PD-L1 mRNA and protein in B16-F10 mouse melanoma cells

To clarify whether inhibition of PD-L1 with EGCG results in stimulation of anti-tumor immunity of T cells, we conducted the co-culture experiment using ovalbumin expressing B16-F10 mouse melanoma cells (F10-OVA cells) and tumor specific CD3+ T cells. Before conduced co-culture experiments, I first examined the effect of IFN-γ, TNF-α, and IL-6 on cell-surface PD-L1 by flow cytometry in B16-F10 cells. Treatment with 50 ng/ml IFN-γ for 24 h, dramatically increased cell-surface PD-L1 level about 19-fold, and 50 ng/ml TNF-α slightly increased 1.5-fold. However, IL-6 did not change the cell-surface PD-L1 level (Figure 20).

Treatment with 10 ng/ml IFN-γ highly enhanced expression of mRNA and cell-surface PD-L1 about 6.5- and 8.5-fold, respectively (Figure 21). Treatment with EGCG at a concentration of 1, 10 and 50 μM inhibited 25%, 69% and 86% of IFN-γ-induced PD-L1 mRNA level, respectively (Figure 21A). Moreover, treatment with EGCG dose-

dependently reduced cell-surface PD-L1 protein level to 7.2- (15% inhibition), 3.1- (63% inhibition) and 1.2-fold (85% inhibition) by 1, 10 and 50 μM EGCG, respectively (Figure 21B). But fludarabine, a STAT1 inhibitor, did not show any inhibition. These results were very similar to lung cancer cell lines. Thus, EGCG inhibited IFN-γ-induced PD-L1 expression at transcriptional levels in mouse melanoma cells similar to human lung cancer cells.

2.3.2.2. EGCG inhibited PD-L1 expression in F10-OVA cells induced by co-cultured with tumor specific CD3+ T cells

Next, I established F10-OVA cells and examined PD-L1 expression in B16-F10-OVA cells (target cells) by co-culture with tumor specific CD3+ T cells (effector cells). I found that cell-surface PD-L1 level in F10-OVA cells was increased 3.7-fold, 48 h after co-culture with tumor specific CD3+ T cells (Figure 22A). Thus, up-regulation of PD-L1 in melanoma cells is triggered by the presence of tumor specific CD3+ T cells.

It is important to note that EGCG reduced PD-L1 mRNA expression induced by co-culture with tumor specific CD3+ T cells. Co-culture of F10-OVA cells with tumor specific CD3+ T cells increased PD-L1 mRNA expression about 1.5-fold compared with that of non-co-cultured F10-OVA cells. Pretreatment with EGCG in F10-OVA cells for 3 h dose-dependently reduced PD-L1 mRNA: 29% reduction by 10 μM EGCG and 40% reduction by 30 μM EGCG, whereas treatment with EGCG in F10-OVA cell alone, did not affect to mRNA PD-L1 in non-co-cultured F10-OVA cells (Figure 22B). These results suggest that EGCG inhibit PD-L1/PD-1 pathway between F10-OVA cells and tumor specific CD3+ T cells.

2.3.2.3 EGCG restored IL-2 mRNA expression in tumor specific CD3+ T cells co-cultured with F10-OVA cells

To clarify whether inhibition of PD-L1 expression in tumor cells with EGCG re-activates T-cell function, I examined the PD-1 mRNA expression in CD3+ T cells co-cultured with F10-OVA cells. The results show that of PD-1 mRNA on T cells slightly increased, and treatment with EGCG showed decrease tendency (Figure 23A), indicating that co-culture with F10-OVA enhanced PD-1 expression in the T cells, and EGCG abrogated it. Next, I examined IL-2 mRNA expression as the marker of activated T cells. Even though the number of T cells are not changed after co-cultured with F10-OVA for 48 h (Figure 23B), IL-2 mRNA expression in co-cultured CD3+ T cells was dramatically decreased by 24% and recovered to about 40% by treatment with EGCG. However, EGCG did not affect IL-2 mRNA expression in non-co-cultured CD3+ T cells (Figure 23C). These results indicate that EGCG restores T-cell activity by suppressing PD-L1/PD-1 inhibitory signaling.

2.3.2.4. EGCG stimulated apoptosis of F10-OVA cells by co-cultured with tumor specific CD3+ T cells

Next, I examined stimulation of CTL activity of tumor specific T cells by induction of apoptosis F10-OVA cells. Percentage of apoptosis cells was determined as sub-G_1-phase cells in cell cycles by flow cytometry. Forty-eight h after co-cultured with tumor specific CD3+ T cells (1:20). Percent of apoptotic cells in F10-OVA was 8.8%, and increased to 19.9% and 34.4% by treatment with 10 and 30 μM EGCG, respectively (Figure 24A). However, treatment with EGCG did not increase % of sub-G_1-phase cells in non-co-culture F10-OVA cells (Figure 24B), indicating that EGCG stimulates CTL

activity of tumor specific CD3+ T cells. Apoptosis of F10-OVA cells was induced by CTL activity. All results clearly indicate that down-regulation of PD-L1 with EGCG in tumor cells restores of T cell function by inhibition of immune escape by the PD-L1/PD-1 pathway.

2.4. Discussion

In this study, I found a new mechanism showing green tea catechin EGCG enhance anti-tumor immune response by inhibition of PD-L1, an immune checkpoint molecule. I first found that oral administration of GTE, which corresponds to green tea beverage consumed by Japanese people every day, reduced PD-L1 positive cells in lung tumors of A/J mice treated with NNK associated with the inhibition of tumor development. Since GTE in drinking water shows the same inhibitory effect on lung tumor development in NNK-treated A/J mice [91], so EGCG and GTE can probably reduce PD-L1 mRNA expression in lung tumors. I did not determine the local concentration of EGCG or catechins in the lung, because EGCG and GTE are easily metabolized in the body and excreted, and some metabolized catechins bound to the proteins. However, based on epidemiological study and a phase II clinical trial in Japan, we know now that drinking 10 cups (120 ml/cup) of green tea per day (equivalent to 2.5 g GTE/day) delays cancer onset and prevents recurrence of colorectal adenomas [11]. Thus, I estimate that the effective amounts for a human correspond to 10 mg GTE/day for a mouse [100]. In this experiment, each mouse took 18 mg GTE/day, about 1.8 times higher than the effective preventive amount of GTE, and the amounts used for the experiments showed reduction of average numbers of tumors per mouse in the NNK + GTE group. Therefore, I concluded that intake of EGCG and catechins by mouse are sufficient to inhibit lung cancer development and PD-L1 expression. Moreover, the co-culture model experiment of F10-OVA (tumor) cells and tumor-specific CD3+ T cells supports that EGCG-mediated-PD-L1-inhibition results in restoration of T-cell activity by suppressing the PD-L1/PD-1 pathway.

EGCG inhibited PD-L1 expression at the transcription level via both

IFNR/JAK2/STAT1 and EGFR/AKT signaling pathways, suggesting that EGCG inhibits IFN-γ-IFNR and EGF-EGFR signaling by inhibiting the ligand-receptor binding [7]. The results are consistent with a recent report that EGCG increased the bending stiffness of artificial lipid membranes by adsorption of galloyl catechin aggregates to the lipid membrane surface [24]. Our group also reported that stiffening of cancer cell membranes with EGCG correlates well with inhibition of EMT, motility and metastasis in lung cancer cells and B16-F10 mouse melanoma cells that cause by the "sealing effects of EGCG" [7,26]. Further studies need to clarify whether EGCG has potential to inhibit binding PD-L1 on the cell membrane of tumors to PD-1 on T cells, similar to inhibition of IFNR and EGFR signaling pathways. It was also reported that EGCG suppressed indoleamine 2,3-dioxygenase (IDO), which can enhance immune escape by blocking IFN-γ-induced JAK/PKC/STAT1 signaling pathway in oral cancer cells [101]. These results strongly indicate that enhancing the effects of EGCG on adaptive immune cells will restrict the growth of tumor cells. Membrane lipid, such as cholesterol, regulates T-cell signaling and function [102], whether EGCG directly enhance T cell function or acts indirectly requires further study.

PD-L1 expression suppresses CTL function by suppressing IL-2 production in melanoma cells [103]. This study showed EGCG inhibited PD-L1 expression induced by co-culture with tumor specific CD3+ T cells in F10-OVA cells. Although, I could not clarify the factor that induced cell-surface PD-L1 expression in this *ex vivo* co-culture, I think that IFN-γ released from T cells is may be the main cytokine to induce PD-L1 expression. It was reported that in co-culture of the CD3+ T cells which were isolated from peripheral blood mononuclear cells (PBMC) of gastric cancer patients produced IFN-γ to induced PD-L1 expression on primary gastric adenocarcinoma epithelial cells,

resulting in promoted T cells apoptosis. And blocking of cell-surface PD-L1 with specific antibody showed reverse T-cell apoptotic effect [104]. In fact, EGCG inhibited IFN-γ-induced PD-L1 expression in mouse melanoma B16-F10 cells similar to lung cancer. Furthermore, EGCG stimulated CTL activity as showing of increase IL-2 mRNA expression in T cells, resulting in apoptosis F10-OVA cells by CTL killing activity probably due to the decrease of PD-L1 expression in *ex vivo* co-culture experiments.

Importantly, EGCG treatment did not directly affect non-co-cultured T cells. Gimzewski's group reported that GTE increased the cell stiffness of tumor cells isolated from the pleural effusion of various cancer patients, but had no effect on normal mesothelial cells [105]. In this experiment, EGCG did not effect on IL-2 induction or T cell number in non-co-cultured CD3+ T cells. Thus, EGCG indirectly enhanced T cells function via inhibition of the PD-L1/PD-1 pathway. Although EGCG can induce apoptosis of cancer cells, EGCG treatment did not directly enhanced apoptosis in non-co-cultured F10-OVA cells: Treatment of EGCG (30 μM) enhanced apoptosis of F10-OVA cells co-cultured with tumor specific CD3+ T cells about 3-fold more than that of F10-OVA cells alone, indicating that EGCG restored CTLs activity via blockade of the PD-L1/PD-1 pathway. It has recently been reported that multiple microRNAs act as important regulators of PD-L1 expression directly or indirectly [106]. Since EGCG up-regulates tumor suppressor microRNAs, it is important to determine whether alteration of microRNAs levels regulated by EGCG inhibits PD-L1 mRNA expression [107].

Expression of tumor cell-associated PD-L1 is induced by overexpression of EGFR and mutation of EGFR in lung cancer cells. Three cell lines used in this experiment do not have any EGFR mutation, but expression levels of EGFR are different: H1299 cells show the lowest, followed by A549 cells (3-fold) and Lu99 cells (10-fold) (Figure

7B and 7C). In addition, Lu99 cells have the mutation of T1025A in PI3K catalytic subunit α (PI3KCA). Therefore, high expression of intrinsic PD-L1 in Lu99 cells may be correlated with high EGFR levels and PI3KCA mutation. Recently, CKLF-like MARVEL transmembrane containing protein 6 (CMTM6) is found as the cell-surface PD-L1 regulator, which maintains cell-surface PD-L1 level [108,109]. I found that CMTM6 mRNA level in Lu99 cells was 1.8-fold higher than those in A549 and H1299 cells (Supplemental Figure 1), and that CMTM6 mRNA level is correlated well with difference of intrinsic PD-L1 expression. Thus, CMTM6 protein probably maintains cell-surface PD-L1 in Lu99 cells, resulting in the weak effect of EGCG treatment. Finding of an inhibitor of CMTM6 and clarify of the regulatory mechanism of cell-surface PD-L1 will be next important subjects.

Recent Phase III clinical trials revealed that the combination of chemotherapy and immune-checkpoint-targeted antibodies show a superior effect than chemotherapy alone, indicating that the use of immune checkpoint inhibitors will likely be extended into cancer treatment [110]. Furthermore, chemotherapy, such as paclitaxel or carboplatin, induce PD-L1 overexpression in ovarian cancer [111]. EGCG and GTE strongly enhanced the efficacy of numerous anti-cancer drugs, including paclitaxel, in various types of cancers *in vitro* and *in vivo* [90]. Since EGCG and GTE are non-toxic, I believe that the inhibitory effects of EGCG on immune checkpoints further support the efficacy of the combination of green tea catechins and anti-cancer drugs.

It is important to note that PD-L1 in tumor cells has additional functions other than immune checkpoint to stimulate cancer progression, such as the promotion of EMT, acquisition of tumor-initiating potential, resistance to apoptosis [112,113]. Interestingly, EGCG and GTE inhibits EMT in lung cancer by increase cell stiffening and inhibit self-

renew of cancer stem cells (tumor-initiating cells) and induce apoptosis of cancer cells [90].

2.5. Conclusion

This dissertation indicates a new concept: Green tea catechin acts as an immune checkpoint inhibitor leading to cancer prevention and treatment. As shown in Figure 25, the "sealing effects of EGCG" causes inhibition of IFN-γ- or EGF-induced PD-L1 expression at transcriptional level, mediated through inhibition of STAT1 or AKT signaling pathway in tumor microenvironment, resulting in restoration of CTLs activity. Specifically, the increase of IL-2 mRNA expression and T-cell proliferation enhance cancer cell apoptosis by EGCG. Thus, EGCG partially restores T-cell activity by inhibition of PD-L1/PD-1 signaling, resulting in inhibition of lung tumor growth.

In 1211, the Japanese Zen priest, Eisai wrote a book entitled "Kitsusa Yojyouki, Maintaining health by drinking green tea," with a famous sentence: Green tea is a wonderful drug for maintaining health, and drinking green tea is an excellent strategy for a long and healthy life, and he concluded that "I am confident that an excellent doctor will elucidate the mechanisms of green tea action in the near future." My study provides new scientific evidence supporting the health benefits of green tea. This new function of EGCG in anti-tumor immune response plays a vital role in combination therapies with green tea catechins and PD-L1 monoclonal antibodies or anticancer drugs, and will further increase benefits for lung cancer therapy.

ABBREVIATIONS

CD3+, cluster of differentiation 3 positive

CTL, cytotoxic T lymphocyte

EC, (-)-epicatechin

ECG, (-)-epicatechin gallate

EGC, (-)-epigallocatechin

EGCG, (-)-epigallocatechin gallate

EGF, epidermal growth factor

EGFR, epidermal growth factor receptor

EMT, epithelial-mesenchymal transition

ERK, extracellular-signal-regulated kinase

F10-OVA, ovalbumin-expressing B16-F10

GTE, green tea extract

IFN-γ, interferon gamma

i.p., intraperitoneal

JAK, Janus kinase

MAPK, mitogen-activated protein kinases

NNK, 4-(methylnitrosamino)-1-(3-pyridyl)-1-butanone

PD-1, programmed cell death 1

PD-L1, programmed cell death-ligand 1

PI3K, phosphoinositide 3-kinase

TPA, 12-*O*-tetradecanoylphorbol-13-acetate

REFERENCES

[1] H. Fujiki, M. Suganuma, K. Imai, K. Nakachi, Green tea: cancer preventive beverage and/or drug, Cancer Lett 188 (2002) 9-13.

[2] M. Pae, D. Wu, Immunomodulating effects of epigallocatechin-3-gallate from green tea: mechanisms and applications, Food Funct 4 (2013) 1287-1303.

[3] H. Fujiki, M. Suttajit, A. Rawangkan, K. Iida, P. Limtrakul, S. Umsumarng, M. Suganuma, Phorbol esters in seed oil of Jatropha curcas L. (saboodam in Thai) and their association with cancer prevention: from the initial investigation to the present topics, J Cancer Res Clin Oncol 143 (2017) 1359-1369.

[4] H. Fujiki, M. Suganuma, Green tea and cancer prevention, Proceedings of the Japan Academy, Series B 78 (2002) 263-270.

[5] H. Fujiki, E. Sueoka, A. Rawangkan, M. Suganuma, Human cancer stem cells are a target for cancer prevention using (−)-epigallocatechin gallate, J Cancer Res Clin Oncol 143 (2017) 2401-2412.

[6] S. Yoshizawa, T. Horiuchi, H. Fujiki, T. Yoshida, T. Okuda, T. Sugimura, Antitumor promoting activity of (−) ‐ epigallocatechin gallate, the main constituent of “Tannin” in green tea, Phytother Res 1 (1987) 44-47.

[7] M. Suganuma, A. Takahashi, T. Watanabe, K. Iida, T. Matsuzaki, H. Yoshikawa, H. Fujiki, Biophysical Approach to Mechanisms of Cancer Prevention and Treatment with Green Tea Catechins, Molecules 21 (2016) 1566.

[8] H. Fujiki, M. Suganuma, K. Imai, K. Nakachi, Green tea: cancer preventive beverage and/or drug, Cancer Letters 188 (2002) 9-13.

[9] M. Suganuma, S. Okabe, M. Oniyama, Y. Tada, H. Ito, H. Fujiki, Wide distribution of

[3H](-)-epigallocatechin gallate, a cancer preventive tea polyphenol, in mouse tissue, Carcinogenesis 19 (1998) 1771-1776.

[10] S. Taniguchi, H. Fujiki, H. Kobayashi, H. Go, K. Miyado, H. Sadano, R. Shimokawa, Effect of (-)-epigallocatechin gallate, the main constituent of green tea, on lung metastasis with mouse B16 melanoma cell lines, Cancer Lett 65 (1992) 51-54.

[11] K. Nakachi, S. Matsuyama, S. Miyake, M. Suganuma, K. Imai, Preventive effects of drinking green tea on cancer and cardiovascular disease: Epidemiological evidence for multiple targeting prevention, BioFactors 13 (2000) 49-54.

[12] K. Imai, K. Suga, K. Nakachi, Cancer-Preventive Effects of Drinking Green Tea among a Japanese Population, Pre Med 26 (1997) 769-775.

[13] K. Nakachi, K. Suemasu, K. Suga, T. Takeo, K. Imai, Y. Higashi, Influence of Drinking Green Tea on Breast Cancer Malignancy among Japanese Patients, Jpn J Cancer Res 89 (1998) 254-261.

[14] M. Shimizu, Y. Fukutomi, M. Ninomiya, K. Nagura, T. Kato, H. Araki, M. Suganuma, H. Fujiki, H. Moriwaki, Green tea extracts for the prevention of metachronous colorectal adenomas: a pilot study, Cancer Epidemiol Biomarkers Prev 17 (2008) 3020-3025.

[15] C.M. Shin, D.H. Lee, A.Y. Seo, H.J. Lee, S.B. Kim, W.C. Son, Y.K. Kim, S.J. Lee, S.H. Park, N. Kim, Y.S. Park, H. Yoon, Green tea extracts for the prevention of metachronous colorectal polyps among patients who underwent endoscopic removal of colorectal adenomas: A randomized clinical trial, Clin Nutr 37 (2018) 452-458.

[16] J.C. Stingl, T. Ettrich, R. Muche, M. Wiedom, J. Brockmoller, A. Seeringer, T. Seufferlein, Protocol for minimizing the risk of metachronous adenomas of the

colorectum with green tea extract (MIRACLE): a randomised controlled trial of green tea extract versus placebo for nutriprevention of metachronous colon adenomas in the elderly population, BMC Cancer 11 (2011) 360.

[17] S. Bettuzzi, M. Brausi, F. Rizzi, G. Castagnetti, G. Peracchia, A. Corti, Chemoprevention of human prostate cancer by oral administration of green tea catechins in volunteers with high-grade prostate intraepithelial neoplasia: a preliminary report from a one-year proof-of-principle study, Cancer Res 66 (2006) 1234-1240.

[18] A.S. Tsao, D. Liu, J. Martin, X.M. Tang, J.J. Lee, A.K. El-Naggar, I. Wistuba, K.S. Culotta, L. Mao, A. Gillenwater, Y.M. Sagesaka, W.K. Hong, V. Papadimitrakopoulou, Phase II randomized, placebo-controlled trial of green tea extract in patients with high-risk oral premalignant lesions, Cancer Prev Res (Phila) 2 (2009) 931-941.

[19] H. Fujiki, E. Sueoka, T. Watanabe, M. Suganuma, Synergistic enhancement of anticancer effects on numerous human cancer cell lines treated with the combination of EGCG, other green tea catechins, and anticancer compounds, J Cancer Res Clin Oncol 141 (2015) 1511-1522.

[20] Y. Oya, A. Mondal, A. Rawangkan, S. Umsumarng, K. Iida, T. Watanabe, M. Kanno, K. Suzuki, Z. Li, H. Kagechika, K. Shudo, H. Fujiki, M. Suganuma, Down-regulation of histone deacetylase 4, −5 and −6 as a mechanism of synergistic enhancement of apoptosis in human lung cancer cells treated with the combination of a synthetic retinoid, Am80 and green tea catechin, J Nutr Biochem 42 (2017) 7-16.

[21] H. Fujiki, Green Tea Cancer Prevention, in: M. Schwab (Ed.), Encyclopedia of

Cancer, Springer Berlin Heidelberg, Berlin, Heidelberg, 2011, pp. 1603-1607.

[22] H. Fujiki, S. Yoshizawa, T. Horiuchi, M. Suganuma, J. Yatsunami, S. Nishiwaki, S. Okabe, R. Nishiwaki-Matsushima, T. Okuda, T. Sugimura, Anticarcinogenic effects of (−)-epigallocatechin gallate, Prev Med 21 (1992) 503-509.

[23] M. Lorenz, Cellular targets for the beneficial actions of tea polyphenols, Am J Clin Nutr 98 (2013) 1642S-1650S.

[24] T. Matsuzaki, H. Ito, V. Chevyreva, A. Makky, S. Kaufmann, K. Okano, N. Kobayashi, M. Suganuma, S. Nakabayashi, H.Y. Yoshikawa, M. Tanaka, Adsorption of galloyl catechin aggregates significantly modulates membrane mechanics in the absence of biochemical cues, Phys Chem Chem Phys 19 (2017) 19937-19947.

[25] K. Iida, R. Sakai, S. Yokoyama, N. Kobayashi, S. Togo, H.Y. Yoshikawa, A. Rawangkan, K. Namiki, M. Suganuma, Cell softening in malignant progression of human lung cancer cells by activation of receptor tyrosine kinase AXL, Sci Rep 7 (2017) 17770.

[26] A. Takahashi, T. Watanabe, A. Mondal, K. Suzuki, M. Kurusu-Kanno, Z. Li, T. Yamazaki, H. Fujiki, M. Suganuma, Mechanism-based inhibition of cancer metastasis with (−)-epigallocatechin gallate, Biochem Biophys Res Commun 443 (2014) 1-6.

[27] T. Matsuzaki, K. Ito, K. Masuda, E. Kakinuma, R. Sakamoto, K. Iketaki, H. Yamamoto, M. Suganuma, N. Kobayashi, S. Nakabayashi, T. Tanii, H.Y. Yoshikawa, Quantitative Evaluation of Cancer Cell Adhesion to Self-Assembled Monolayer-Patterned Substrates by Reflection Interference Contrast Microscopy, J Phys Chem B 120 (2016) 1221-1227.

[28] V. Naponelli, I. Ramazzina, C. Lenzi, S. Bettuzzi, F. Rizzi, Green Tea Catechins for Prostate Cancer Prevention: Present Achievements and Future Challenges, Antioxidants 6 (2017) 26.

[29] S. Adachi, T. Nagao, H.I. Ingolfsson, F.R. Maxfield, O.S. Andersen, L. Kopelovich, I.B. Weinstein, The inhibitory effect of (-)-epigallocatechin gallate on activation of the epidermal growth factor receptor is associated with altered lipid order in HT29 colon cancer cells, Cancer Res 67 (2007) 6493-6501.

[30] S. Adachi, T. Nagao, S. To, A.K. Joe, M. Shimizu, R. Matsushima-Nishiwaki, O. Kozawa, H. Moriwaki, F.R. Maxfield, I.B. Weinstein, (-)-Epigallocatechin gallate causes internalization of the epidermal growth factor receptor in human colon cancer cells, Carcinogenesis 29 (2008) 1986-1993.

[31] Y. Ishida, Y. Agata, K. Shibahara, T. Honjo, Induced expression of PD-1, a novel member of the immunoglobulin gene superfamily, upon programmed cell death, EMBO J 11 (1992) 3887-3895.

[32] K.M. Mahoney, G.J. Freeman, D.F. McDermott, The Next Immune-Checkpoint Inhibitors: PD-1/PD-L1 Blockade in Melanoma, Clin Ther 37 (2015) 764-782.

[33] L. Shi, S. Chen, L. Yang, Y. Li, The role of PD-1 and PD-L1 in T-cell immune suppression in patients with hematological malignancies, J Hematol Oncol 6 (2013) 74-74.

[34] H. Dong, G. Zhu, K. Tamada, L. Chen, B7-H1, a third member of the B7 family, co-stimulates T-cell proliferation and interleukin-10 secretion, Nat Med 5 (1999) 1365.

[35] Y. Latchman, C.R. Wood, T. Chernova, D. Chaudhary, M. Borde, I. Chernova, Y. Iwai, A.J. Long, J.A. Brown, R. Nunes, E.A. Greenfield, K. Bourque, V.A.

Boussiotis, L.L. Carter, B.M. Carreno, N. Malenkovich, H. Nishimura, T. Okazaki, T. Honjo, A.H. Sharpe, G.J. Freeman, PD-L2 is a second ligand for PD-1 and inhibits T cell activation, Nat Immunol 2 (2001) 261.

[36] M. Ishida, Y. Iwai, Y. Tanaka, T. Okazaki, G.J. Freeman, N. Minato, T. Honjo, Differential expression of PD-L1 and PD-L2, ligands for an inhibitory receptor PD-1, in the cells of lymphohematopoietic tissues, Immunol Lett 84 (2002) 57-62.

[37] T. Yamazaki, H. Akiba, H. Iwai, H. Matsuda, M. Aoki, Y. Tanno, T. Shin, H. Tsuchiya, D.M. Pardoll, K. Okumura, M. Azuma, H. Yagita, Expression of Programmed Death 1 Ligands by Murine T Cells and APC, Immunol 169 (2002) 5538.

[38] H. Yu, T.A. Boyle, C. Zhou, D.L. Rimm, F.R. Hirsch, PD-L1 Expression in Lung Cancer, J Thorac Oncol 11 (2016) 964-975.

[39] J. He, Y. Hu, M. Hu, B. Li, Development of PD-1/PD-L1 Pathway in Tumor Immune Microenvironment and Treatment for Non-Small Cell Lung Cancer, Sci Rep 5 (2015) 13110.

[40] S. Maleki Vareki, C. Garrigós, I. Duran, Biomarkers of response to PD-1/PD-L1 inhibition, Crit Rev Oncol Hematol 116 (2017) 116-124.

[41] H. Dong, S.E. Strome, D.R. Salomao, H. Tamura, F. Hirano, D.B. Flies, P.C. Roche, J. Lu, G. Zhu, K. Tamada, V.A. Lennon, E. Celis, L. Chen, Tumor-associated B7-H1 promotes T-cell apoptosis: A potential mechanism of immune evasion, Nat Med 8 (2002) 793.

[42] G.J. Freeman, A.H. Sharpe, V.K. Kuchroo, Protect the killer: CTLs need defenses against the tumor, Nat Med 8 (2002) 787.

[43] J. Hamanishi, M. Mandai, N. Matsumura, K. Abiko, T. Baba, I. Konishi, PD-1/PD-L1 blockade in cancer treatment: perspectives and issues, Int J Clin Oncol 21

(2016) 462-473.

[44] R. Pichler, I. Heidegger, J. Fritz, M. Danzl, S. Sprung, B. Zelger, A. Brunner, A. Pircher, PD-L1 expression in bladder cancer and metastasis and its influence on oncologic outcome after cystectomy, Oncotarget 8 (2017) 66849-66864.

[45] J. Long, J. Lin, A. Wang, L. Wu, Y. Zheng, X. Yang, X. Wan, H. Xu, S. Chen, H. Zhao, PD-1/PD-L blockade in gastrointestinal cancers: lessons learned and the road toward precision immunotherapy, J Hematol Oncol 10 (2017) 146.

[46] E.A. Mittendorf, A.V. Philips, F. Meric-Bernstam, N. Qiao, Y. Wu, S. Harrington, X. Su, Y. Wang, A.M. Gonzalez-Angulo, A. Akcakanat, A. Chawla, M. Curran, P. Hwu, P. Sharma, J.K. Litton, J.J. Molldrem, G. Alatrash, PD-L1 Expression in Triple-Negative Breast Cancer, Cancer Immunol Res 2 (2014) 361-370.

[47] K.K. Tsai, I. Zarzoso, A.I. Daud, PD-1 and PD-L1 antibodies for melanoma, Hum Vaccin Immunother 10 (2014) 3111-3116.

[48] K. Abiko, N. Matsumura, J. Hamanishi, N. Horikawa, R. Murakami, K. Yamaguchi, Y. Yoshioka, T. Baba, I. Konishi, M. Mandai, IFN-γ from lymphocytes induces PD-L1 expression and promotes progression of ovarian cancer, Br J Cancer 112 (2015) 1501.

[49] J. Hamanishi, M. Mandai, I. Konishi, Immune checkpoint inhibition in ovarian cancer, Int Immunol 28 (2016) 339-348.

[50] Y.K. Chae, A. Pan, A.A. Davis, K. Raparia, N.A. Mohindra, M. Matsangou, F.J. Giles, Biomarkers for PD-1/PD-L1 Blockade Therapy in Non–Small-cell Lung Cancer: Is PD-L1 Expression a Good Marker for Patient Selection?, Clin Lung Cancer 17 (2016) 350-361.

[51] W. Jing, M. Li, Y. Zhang, F. Teng, A. Han, L. Kong, H. Zhu, PD-1/PD-L1 blockades

in non-small-cell lung cancer therapy, OncoTargets Ther 9 (2016) 489-502.

[52] M. Zhang, G. Li, Y. Wang, Y. Wang, S. Zhao, P. Haihong, H. Zhao, Y. Wang, PD-L1 expression in lung cancer and its correlation with driver mutations: a meta-analysis, Sci Rep 7 (2017) 10255.

[53] J.R. Webb, K. Milne, D.R. Kroeger, B.H. Nelson, PD-L1 expression is associated with tumor-infiltrating T cells and favorable prognosis in high-grade serous ovarian cancer, Gynecol Oncol 141 (2016) 293-302.

[54] A. Garcia-Diaz, D.S. Shin, B.H. Moreno, J. Saco, H. Escuin-Ordinas, G.A. Rodriguez, J.M. Zaretsky, L. Sun, W. Hugo, X. Wang, G. Parisi, C.P. Saus, D.Y. Torrejon, T.G. Graeber, B. Comin-Anduix, S. Hu-Lieskovan, R. Damoiseaux, R.S. Lo, A. Ribas, Interferon Receptor Signaling Pathways Regulating PD-L1 and PD-L2 Expression, Cell Rep 19 (2017) 1189-1201.

[55] M. Kousaku, T.J. Liang, O. Hirokazu, S. Kensuke, K. Ley‐Fang, K. Vivien, S.D. T., A. Hassan, O. Takahiro, S. Yoshiyuki, F. Zul, A.B. R., S. Asim, Y. Wei‐Peng, S. Jimmy, S. Richie, K. Koji, PD‐L1 expression is mainly regulated by interferon gamma associated with JAK‐STAT pathway in gastric cancer, Cancer Sci 109 (2018) 43-53.

[56] S. Ikeda, T. Okamoto, S. Okano, Y. Umemoto, T. Tagawa, Y. Morodomi, M. Kohno, S. Shimamatsu, H. Kitahara, Y. Suzuki, T. Fujishita, Y. Maehara, PD-L1 Is Upregulated by Simultaneous Amplification of the PD-L1 and JAK2 Genes in Non–Small Cell Lung Cancer, J Thorac Oncol 11 (2016) 62-71.

[57] X. Wang, L. Yang, F. Huang, Q. Zhang, S. Liu, L. Ma, Z. You, Inflammatory cytokines IL-17 and TNF-α up-regulate PD-L1 expression in human prostate and colon cancer cells, Immunol Lett 184 (2017) 7-14.

[58] W. Zhang, Q. Pang, C. Yan, Q. Wang, J. Yang, S. Yu, X. Liu, Z. Yuan, P. Wang, Z. Xiao, Induction of PD-L1 expression by epidermal growth factor receptor–mediated signaling in esophageal squamous cell carcinoma, OncoTargets Ther 10 (2017) 763-771.

[59] I.B. Barsoum, C.A. Smallwood, D.R. Siemens, C.H. Graham, A Mechanism of Hypoxia-Mediated Escape from Adaptive Immunity in Cancer Cells, Cancer Res 74 (2014) 665.

[60] K.J. Lastwika, W. Wilson, Q.K. Li, J. Norris, H. Xu, S.R. Ghazarian, H. Kitagawa, S. Kawabata, J.M. Taube, S. Yao, L.N. Liu, J.J. Gills, P.A. Dennis, Control of PD-L1 Expression by Oncogenic Activation of the AKT–mTOR Pathway in Non–Small Cell Lung Cancer, Cancer Res 76 (2016) 227-238.

[61] S. Kleffel, C. Posch, Steven R. Barthel, H. Mueller, C. Schlapbach, E. Guenova, Christopher P. Elco, N. Lee, Vikram R. Juneja, Q. Zhan, Christine G. Lian, R. Thomi, W. Hoetzenecker, A. Cozzio, R. Dummer, Martin C. Mihm, Keith T. Flaherty, Markus H. Frank, George F. Murphy, Arlene H. Sharpe, Thomas S. Kupper, T. Schatton, Melanoma Cell-Intrinsic PD-1 Receptor Functions Promote Tumor Growth, Cell 162 (2015) 1242-1256.

[62] J. Gong, A. Chehrazi-Raffle, S. Reddi, R. Salgia, Development of PD-1 and PD-L1 inhibitors as a form of cancer immunotherapy: a comprehensive review of registration trials and future considerations, J ImmunoTher Cancer 6 (2018) 8.

[63] H.T. Lee, J.Y. Lee, H. Lim, S.H. Lee, Y.J. Moon, H.J. Pyo, S.E. Ryu, W. Shin, Y.-S. Heo, Molecular mechanism of PD-1/PD-L1 blockade via anti-PD-L1 antibodies atezolizumab and durvalumab, Sci Rep 7 (2017) 5532.

[64] A.H. Sharpe, K.E. Pauken, The diverse functions of the PD1 inhibitory pathway, Nat

Rev Immunol 18 (2017) 153.

[65] C. Robert, G.V. Long, B. Brady, C. Dutriaux, M. Maio, L. Mortier, J.C. Hassel, P. Rutkowski, C. McNeil, E. Kalinka-Warzocha, K.J. Savage, M.M. Hernberg, C. Lebbé, J. Charles, C. Mihalcioiu, V. Chiarion-Sileni, C. Mauch, F. Cognetti, A. Arance, H. Schmidt, D. Schadendorf, H. Gogas, L. Lundgren-Eriksson, C. Horak, B. Sharkey, I.M. Waxman, V. Atkinson, P.A. Ascierto, Nivolumab in Previously Untreated Melanoma without BRAF Mutation, N Engl J Med 372 (2015) 320-330.

[66] C. Nicolazzo, C. Raimondi, M. Mancini, S. Caponnetto, A. Gradilone, O. Gandini, M. Mastromartino, G. del Bene, A. Prete, F. Longo, E. Cortesi, P. Gazzaniga, Monitoring PD-L1 positive circulating tumor cells in non-small cell lung cancer patients treated with the PD-1 inhibitor Nivolumab, Sci Rep 6 (2016) 31726.

[67] M. Reck, D. Rodríguez-Abreu, A.G. Robinson, R. Hui, T. Csőszi, A. Fülöp, M. Gottfried, N. Peled, A. Tafreshi, S. Cuffe, M. O'Brien, S. Rao, K. Hotta, M.A. Leiby, G.M. Lubiniecki, Y. Shentu, R. Rangwala, J.R. Brahmer, Pembrolizumab versus Chemotherapy for PD-L1–Positive Non–Small-Cell Lung Cancer, N Engl J Med 375 (2016) 1823-1833.

[68] I. Funatogawa, T. Funatogawa, E. Yano, Trends in smoking and lung cancer mortality in Japan, by birth cohort, 1949–2010, Bull World Health Organ 91 (2013) 332-340.

[69] A.H. Scheel, S. Ansen, A.M. Schultheis, M. Scheffler, R.N. Fischer, S. Michels, M. Hellmich, J. George, T. Zander, M. Brockmann, E. Stoelben, H. Groen, W. Timens, S. Perner, M. von Bergwelt-Baildon, R. Buttner, J. Wolf, PD-L1 expression in non-small cell lung cancer: Correlations with genetic alterations, Oncoimmunology 5 (2016) e1131379.

[70] M.K. Yeo, S.Y. Choi, I.O. Seong, K.S. Suh, J.M. Kim, K.H. Kim, Association of PD-L1 expression and PD-L1 gene polymorphism with poor prognosis in lung adenocarcinoma and squamous cell carcinoma, Hum Pathol 68 (2017) 103-111.

[71] A. Calles, X. Liao, L.M. Sholl, S.J. Rodig, G.J. Freeman, M. Butaney, C. Lydon, S.E. Dahlberg, F.S. Hodi, G.R. Oxnard, D.M. Jackman, P.A. Jänne, Expression of PD-1 and Its Ligands, PD-L1 and PD-L2, in Smokers and Never Smokers with KRAS-Mutant Lung Cancer, J Thorac Oncol 10 (2015) 1726-1735.

[72] R. Okita, A. Maeda, K. Shimizu, Y. Nojima, S. Saisho, M. Nakata, PD-L1 overexpression is partially regulated by EGFR/HER2 signaling and associated with poor prognosis in patients with non-small-cell lung cancer, Cancer Immunol Immunother 66 (2017) 865-876.

[73] P. Ritprajak, M. Azuma, Intrinsic and extrinsic control of expression of the immunoregulatory molecule PD-L1 in epithelial cells and squamous cell carcinoma, Oral Oncol 51 (2015) 221-228.

[74] N. Chen, W. Fang, Z. Lin, P. Peng, J. Wang, J. Zhan, S. Hong, J. Huang, L. Liu, J. Sheng, T. Zhou, Y. Chen, H. Zhang, L. Zhang, KRAS mutation-induced upregulation of PD-L1 mediates immune escape in human lung adenocarcinoma, Cancer Immunol Immunother 66 (2017) 1175-1187.

[75] A. Minchom, P. Thavasu, Z. Ahmad, A. Stewart, A. Georgiou, M.E.R. O'Brien, S. Popat, J. Bhosle, T.A. Yap, J. de Bono, U. Banerji, A study of PD-L1 expression in KRAS mutant non-small cell lung cancer cell lines exposed to relevant targeted treatments, PLoS One 12 (2017) e0186106.

[76] N. Chen, W. Fang, J. Zhan, S. Hong, Y. Tang, S. Kang, Y. Zhang, X. He, T. Zhou, T. Qin, Y. Huang, X. Yi, L. Zhang, Upregulation of PD-L1 by EGFR Activation

Mediates the Immune Escape in EGFR-Driven NSCLC: Implication for Optional Immune Targeted Therapy for NSCLC Patients with EGFR Mutation, J Thorac Oncol 10 (2015) 910-923.

[77] G.Z. Ge, T.R. Xu, C. Chen, Tobacco carcinogen NNK-induced lung cancer animal models and associated carcinogenic mechanisms, Acta Biochim Biophys Sin (Shanghai) 47 (2015) 477-487.

[78] Z. Sun, Z. Xiao, 4-(Methylnitrosamino)-1-(3-pyridyl)-1-butanone (NNK) regulates CTL activation and memory programming, Biochem Biophys Res Commun 435 (2013) 472-476.

[79] R. Bellucci, A. Martin, D. Bommarito, K. Wang, S.H. Hansen, G.J. Freeman, J. Ritz, Interferon-gamma-induced activation of JAK1 and JAK2 suppresses tumor cell susceptibility to NK cells through upregulation of PD-L1 expression, Oncoimmunology 4 (2015) e1008824.

[80] A. Garcia-Diaz, D.S. Shin, B.H. Moreno, J. Saco, H. Escuin-Ordinas, G.A. Rodriguez, J.M. Zaretsky, L. Sun, W. Hugo, X. Wang, G. Parisi, C.P. Saus, D.Y. Torrejon, T.G. Graeber, B. Comin-Anduix, S. Hu-Lieskovan, R. Damoiseaux, R.S. Lo, A. Ribas, Interferon Receptor Signaling Pathways Regulating PD-L1 and PD-L2 Expression, Cell Rep 19 (2017) 1189-1201.

[81] S. Ikeda, T. Okamoto, S. Okano, Y. Umemoto, T. Tagawa, Y. Morodomi, M. Kohno, S. Shimamatsu, H. Kitahara, Y. Suzuki, T. Fujishita, Y. Maehara, PD-L1 Is Upregulated by Simultaneous Amplification of the PD-L1 and JAK2 Genes in Non-Small Cell Lung Cancer, J Thorac Oncol 11 (2016) 62-71.

[82] S.H. Baumeister, G.J. Freeman, G. Dranoff, A.H. Sharpe, Coinhibitory Pathways in Immunotherapy for Cancer, Annu Rev Immunol 34 (2016) 539-573.

[83] Y. Dong, Q. Sun, X. Zhang, PD-1 and its ligands are important immune checkpoints in cancer, Oncotarget 8 (2017) 2171-2186.

[84] Z. Liang, Y. Tian, W. Cai, Z. Weng, Y. Li, H. Zhang, Y. Bao, Y. Li, High-affinity human PD-L1 variants attenuate the suppression of T cell activation, Oncotarget 8 (2017) 88360-88375.

[85] M.R.P. Coombs, M.E. Harrison, D.W. Hoskin, Apigenin inhibits the inducible expression of programmed death ligand 1 by human and mouse mammary carcinoma cells, Cancer Lett 380 (2016) 424-433.

[86] N. Seetharamu, I.R. Preeshagul, K.M. Sullivan, New PD-L1 inhibitors in non-small cell lung cancer – impact of atezolizumab, Lung Cancer (Auckl) 8 (2017) 67-78.

[87] X. Meng, Y. Liu, J. Zhang, F. Teng, L. Xing, J. Yu, PD-1/PD-L1 checkpoint blockades in non-small cell lung cancer: New development and challenges, Cancer Lett 405 (2017) 29-37.

[88] H. Zhu, F. Bengsch, N. Svoronos, Melanie R. Rutkowski, Benjamin G. Bitler, Michael J. Allegrezza, Y. Yokoyama, Andrew V. Kossenkov, James E. Bradner, Jose R. Conejo-Garcia, R. Zhang, BET Bromodomain Inhibition Promotes Anti-tumor Immunity by Suppressing PD-L1 Expression, Cell Rep 16 (2016) 2829-2837.

[89] Z. Hu, L. Ye, Y. Xing, J. Hu, T. Xi, Combined SEP and anti-PD-L1 antibody produces a synergistic antitumor effect in B16-F10 melanoma-bearing mice, Sci Rep 8 (2018) 217.

[90] H. Fujiki, T. Watanabe, E. Sueoka, A. Rawangkan, M. Suganuma, Cancer Prevention with Green Tea and Its Principal Constituent, EGCG: from Early Investigations to Current Focus on Human Cancer Stem Cells, Mol. Cells 41 (2018) 73-82.

[91] Y. Xu, C.T. Ho, S.G. Amin, C. Han, F.L. Chung, Inhibition of tobacco-specific nitrosamine-induced lung tumorigenesis in A/J mice by green tea and its major polyphenol as antioxidants, Cancer Res 52 (1992) 3875-3879.

[92] T. Kuzuhara, Y. Sei, K. Yamaguchi, M. Suganuma, H. Fujiki, DNA and RNA as new binding targets of green tea catechins, J Biol Chem 281 (2006) 17446-17456.

[93] A. Ribas, J.D. Wolchok, Cancer immunotherapy using checkpoint blockade, Science 359 (2018) 1350-1355.

[94] S.H. Baumeister, G.J. Freeman, G. Dranoff, A.H. Sharpe, Coinhibitory Pathways in Immunotherapy for Cancer, Annu Rev Immunol 34 (2016) 539-573.

[95] E.A. Akbay, S. Koyama, J. Carretero, A. Altabef, J.H. Tchaicha, C.L. Christensen, O.R. Mikse, A.D. Cherniack, E.M. Beauchamp, T.J. Pugh, M.D. Wilkerson, P.E. Fecci, M. Butaney, J.B. Reibel, M. Soucheray, T.J. Cohoon, P.A. Janne, M. Meyerson, D.N. Hayes, G.I. Shapiro, T. Shimamura, L.M. Sholl, S.J. Rodig, G.J. Freeman, P.S. Hammerman, G. Dranoff, K.K. Wong, Activation of the PD-1 pathway contributes to immune escape in EGFR-driven lung tumors, Cancer Discov 3 (2013) 1355-1363.

[96] I.B. Barsoum, C.A. Smallwood, D.R. Siemens, C.H. Graham, A mechanism of hypoxia-mediated escape from adaptive immunity in cancer cells, Cancer Res 74 (2014) 665-674.

[97] M. Suganuma, A. Saha, H. Fujiki, New cancer treatment strategy using combination of green tea catechins and anticancer drugs, Cancer Sci 102 (2011) 317-323.

[98] Y. Xu, C.-T. Ho, S.G. Amin, C. Han, F.-L. Chung, Inhibition of Tobacco-specific Nitrosamine-induced Lung Tumorigenesis in A/J Mice by Green Tea and Its Major Polyphenol as Antioxidants, Cancer Res 52 (1992) 3875.

[99] P. Devanand, Y. Oya, S. Sundaramoorthy, K.Y. Song, T. Watanabe, Y. Kobayashi, Y. Shimizu, S.A. Hong, M. Suganuma, I.K. Lim, Inhibition of TNFalpha-interacting protein alpha (Tipalpha)-associated gastric carcinogenesis by BTG2(/TIS21) via downregulating cytoplasmic nucleolin expression, Exp Mol Med 50 (2018) e449.

[100] A.B. Nair, S. Jacob, A simple practice guide for dose conversion between animals and human, J Basic Clin Pharm 7 (2016) 27-31.

[101] C.W. Cheng, P.C. Shieh, Y.C. Lin, Y.J. Chen, Y.H. Lin, D.H. Kuo, J.Y. Liu, J.Y. Kao, M.C. Kao, T.D. Way, Indoleamine 2,3-dioxygenase, an immunomodulatory protein, is suppressed by (-)-epigallocatechin-3-gallate via blocking of gamma-interferon-induced JAK-PKC-delta-STAT1 signaling in human oral cancer cells, J Agric Food Chem 58 (2010) 887-894.

[102] A. Bietz, H. Zhu, M. Xue, C. Xu, Cholesterol Metabolism in T Cells, Front Immunol 8 (2017) 1664.

[103] W. Yang, P.W. Chen, H. Li, H. Alizadeh, J.Y. Niederkorn, PD-L1: PD-1 interaction contributes to the functional suppression of T-cell responses to human uveal melanoma cells in vitro, Invest Ophthalmol Vis Sci 49 (2008) 2518-2525.

[104] Y.M. Chiu, C.L. Tsai, J.T. Kao, C.T. Hsieh, D.C. Shieh, Y.J. Lee, G.J. Tsay, K.S. Cheng, Y.Y. Wu, PD-1 and PD-L1 Up-regulation Promotes T-cell Apoptosis in Gastric Adenocarcinoma, Anticancer Res 38 (2018) 2069-2078.

[105] S.E. Cross, Y.-S. Jin, J. Rao, J.K. Gimzewski, Nanomechanical analysis of cells from cancer patients, Nat Nanotechnol 2 (2007) 780.

[106] Q. Wang, W. Lin, X. Tang, S. Li, L. Guo, Y. Lin, H.F. Kwok, The Roles of microRNAs in Regulating the Expression of PD-1/PD-L1 Immune Checkpoint, Int J Mol Sci 18 (2017).

[107] S. Sethi, Y. Li, F.H. Sarkar, Regulating miRNA by Natural Agents as a New Strategy for Cancer Treatment, Curr drug targets 14 (2013) 1167-1174.

[108] M.L. Burr, C.E. Sparbier, Y.-C. Chan, J.C. Williamson, K. Woods, P.A. Beavis, E.Y.N. Lam, M.A. Henderson, C.C. Bell, S. Stolzenburg, O. Gilan, S. Bloor, T. Noori, D.W. Morgens, M.C. Bassik, P.J. Neeson, A. Behren, P.K. Darcy, S.-J. Dawson, I. Voskoboinik, J.A. Trapani, J. Cebon, P.J. Lehner, M.A. Dawson, CMTM6 maintains the expression of PD-L1 and regulates anti-tumour immunity, Nature 549 (2017) 101.

[109] R. Mezzadra, C. Sun, L.T. Jae, R. Gomez-Eerland, E. de Vries, W. Wu, M.E.W. Logtenberg, M. Slagter, E.A. Rozeman, I. Hofland, A. Broeks, H.M. Horlings, L.F.A. Wessels, C.U. Blank, Y. Xiao, A.J.R. Heck, J. Borst, T.R. Brummelkamp, T.N.M. Schumacher, Identification of CMTM6 and CMTM4 as PD-L1 protein regulators, Nature 549 (2017) 106.

[110] L. Hendriks, B. Besse, New windows open for immunotherapy in lung cancer, Nature 558 (2018) 376-377.

[111] J. Peng, J. Hamanishi, N. Matsumura, K. Abiko, K. Murat, T. Baba, K. Yamaguchi, N. Horikawa, Y. Hosoe, S.K. Murphy, I. Konishi, M. Mandai, Chemotherapy Induces Programmed Cell Death-Ligand 1 Overexpression via the Nuclear Factor-kappaB to Foster an Immunosuppressive Tumor Microenvironment in Ovarian Cancer, Cancer Res 75 (2015) 5034-5045.

[112] L. Chen, Y. Xiong, J. Li, X. Zheng, Q. Zhou, A. Turner, C. Wu, B. Lu, J. Jiang, PD-L1 Expression Promotes Epithelial to Mesenchymal Transition in Human Esophageal Cancer, Cellular Physiology and Biochemistry 42 (2017) 2267-2280.

[113] F. Zheng, J. Dang, H. Zha, B. Zhang, M. Lin, F. Cheng, PD-L1 Promotes Self-

Renewal and Tumorigenicity of Malignant Melanoma Initiating Cells, BioMed Res Int 2017 (2017) 8.

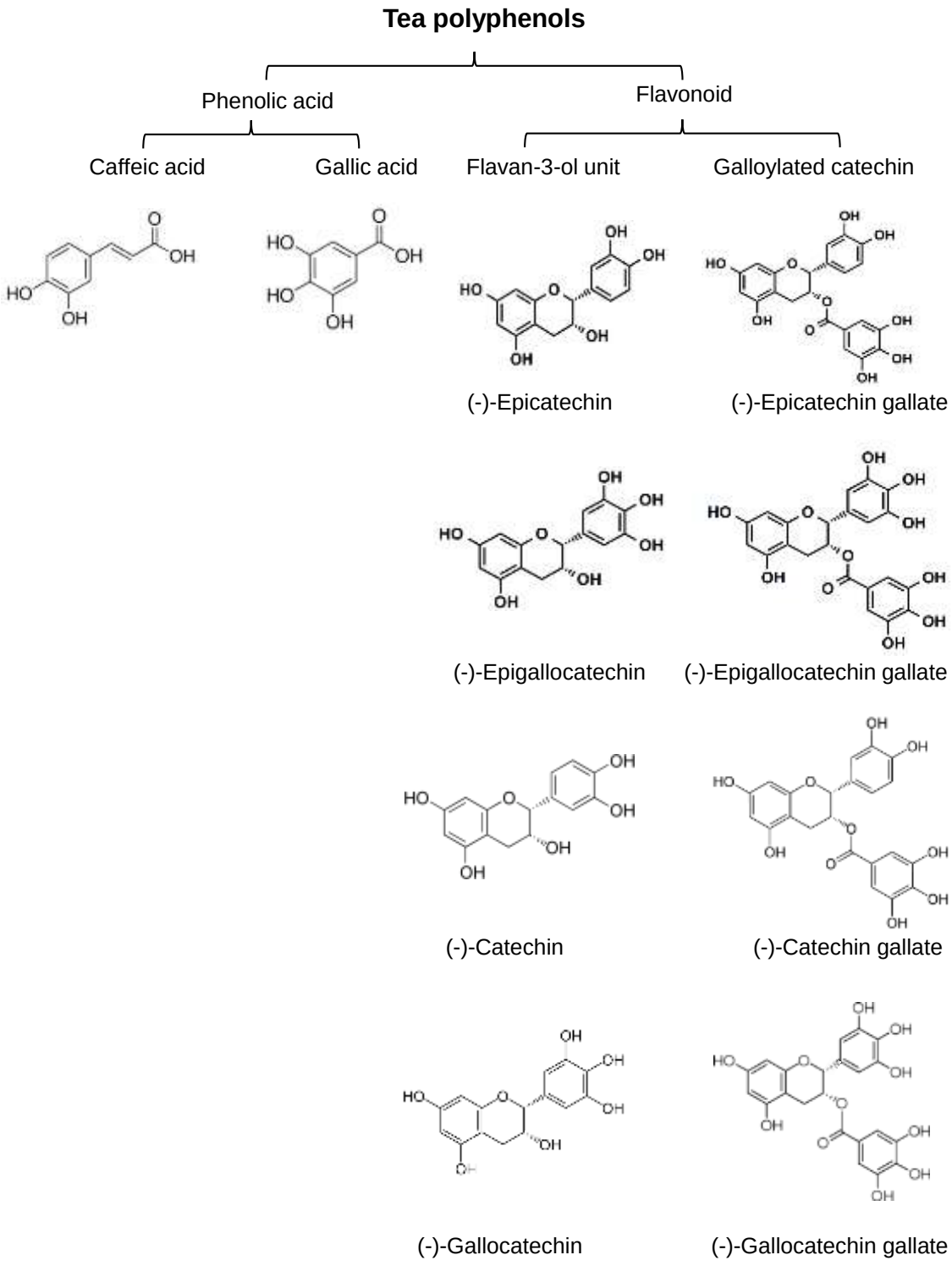

Figure 1. Chemical structures and classifications of tea polyphenols

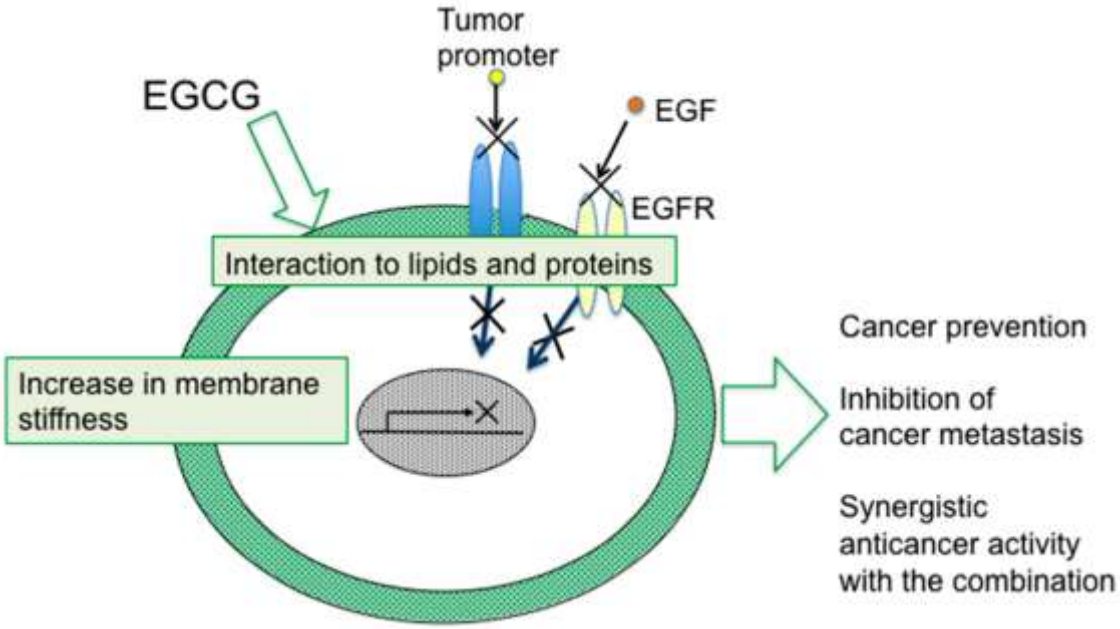

Figure 2. A schematic illustration of the mechanisms of action of EGCG, the "sealing effects of EGCG" [7].

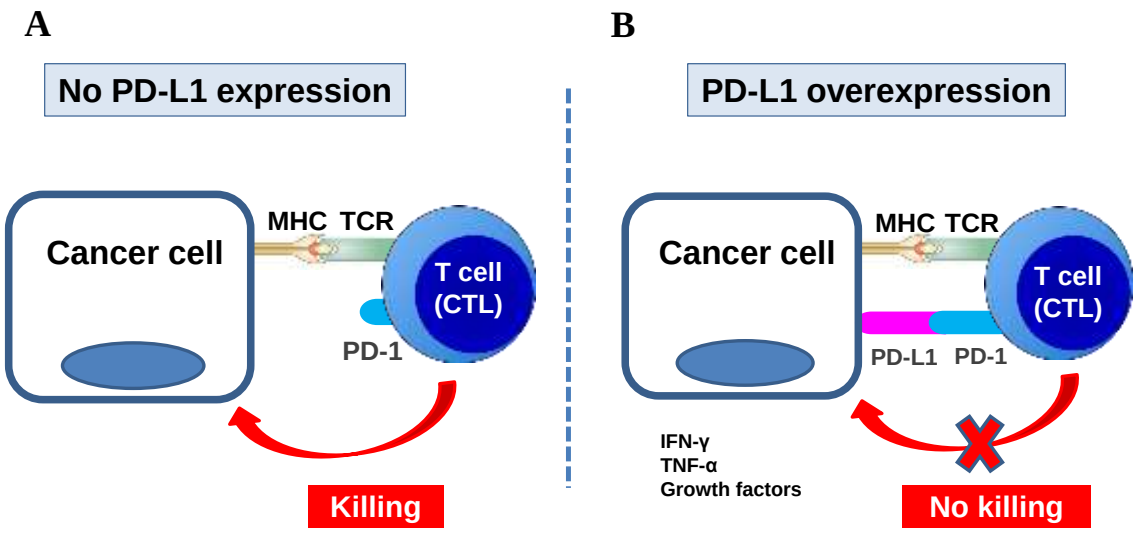

TCR: T cell receptor

CTL: Cytotoxic T lymphocytes

MHC: Major Histocompatibility Complex

Figure 3. Cancer uses PD-L1 for immune escape. In inflammatory tumor microenvironment, various cancer cells overexpress PD-L1 induced by proinflammatory cytokines, such as IFN-γ, TNF-α, and growth factors. (A) Cancer cell without PD-L1 expression, cytotoxic T lymphocytes are activated after recognized the tumor antigen on MHC by T cell receptor (TCR) and kill cancer cells. (B) Cancer over cell overexpressing PD-L1 escape from T cell immune response by binding of PD-L1 to PD-1.

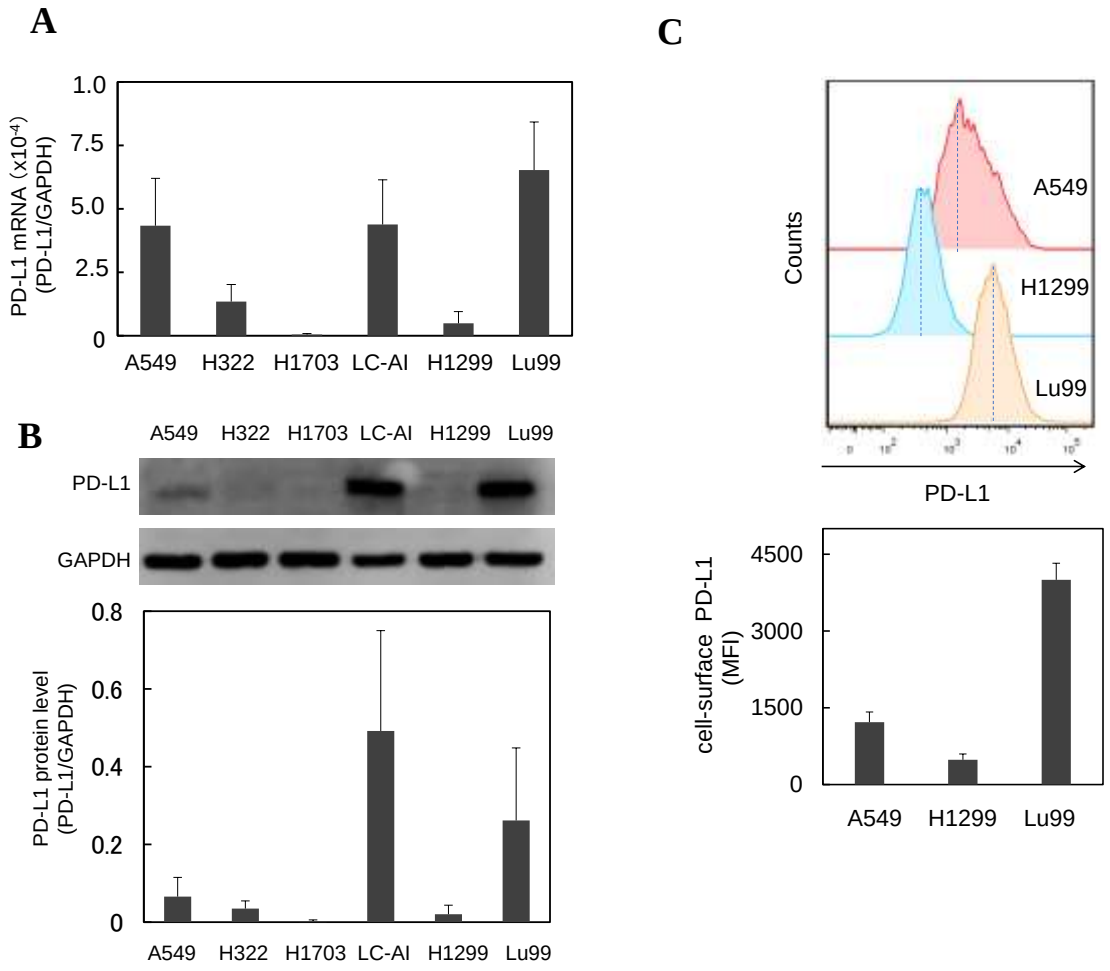

Figure 4. Intrinsic PD-L1 expression levels varied among NSCLCs. (A) PD-L1 mRNA levels in six NSCLCs were measured by qRT-PCR. (B) PD-L1 protein level was detected by western blotting with specific antibodies against PD-L1 and GAPDH, then quantified the density of each band. Lower graph indicates relative PD-L1 protein level normalized by GAPDH as an internal control. (C) The cell-surface PD-L1 level was examined by flow cytometry and measured fluorescence intensity (MFI) of total 10,000 cells as described in Materials and Methods. A dotted line indicates an average of MFI. Cell-surface PD-L1 values were calculated an average of MFI by subtracting the appropriate control value. All data were performed in three independent experiments; ± SD.

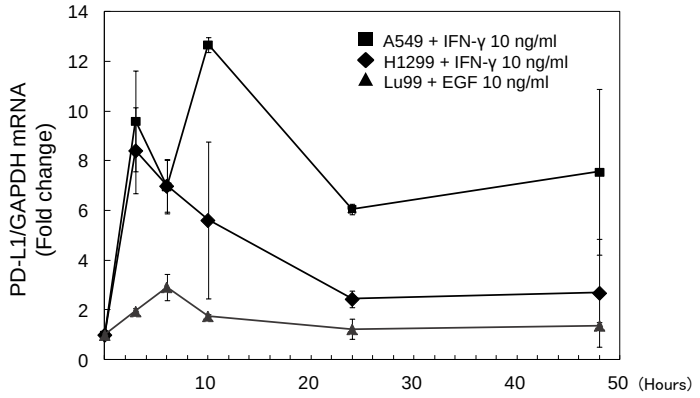

Figure 5. Time-cause of PD-L1 mRNA expression treated with IFN-γ in A549 and H1299 cells or with EGF in Lu99 cells. A549 and H1299 cells were treated with 10 ng/ml IFN-γ, and Lu99 cells were treated with 10 ng/ml EGF. Fold-change of PD-L1/GAPDH mRNA level was measured at 0, 3, 6, 10, 24 and 48 h after treatment. Error bars show ± SD in three different experiments.

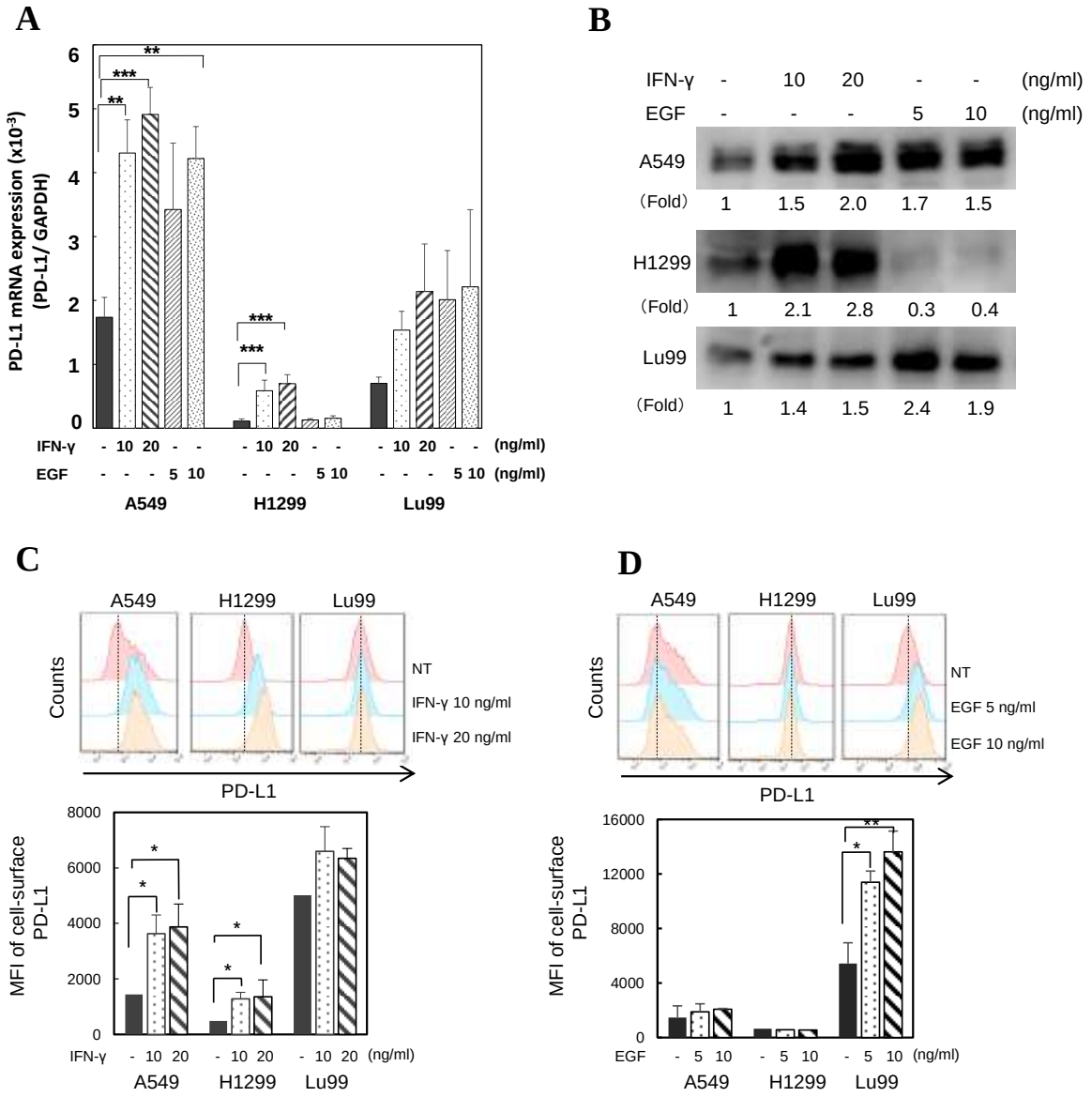

Figure 6. IFN-γ and EGF induced expression of PD-L1 mRNA and protein in NSCLC cell lines. A549, H1299, and Lu99 cells were treated with IFN-γ 10 or 20 ng/ml as well as EGF 5 or 10 ng/ml for 24 h in appropriated medium containing with 1% FBS medium. (A) Expression of PD-L1 mRNA in three cell lines determined by qRT-PCR. (B) The representative protein level of PD-L1 examined by western blotting. Numbers indicate fold-change compared with non-treated cells. (C) Cell-surface PD-L1 in three cell lines treated with IFN-γ for 24 h and (D) cell-surface PD-L1 in three cell lines treated with EGF for 24 h, determined by flow cytometry. The average MFI ± SD was obtained by combining the data from three independent experiments. *$p < 0.05$, **$p < 0.01$, ***$p < 0.001$, by one-way ANOVA followed by Dunnett's Multiple Comparisons Test. NT; non-treated cells

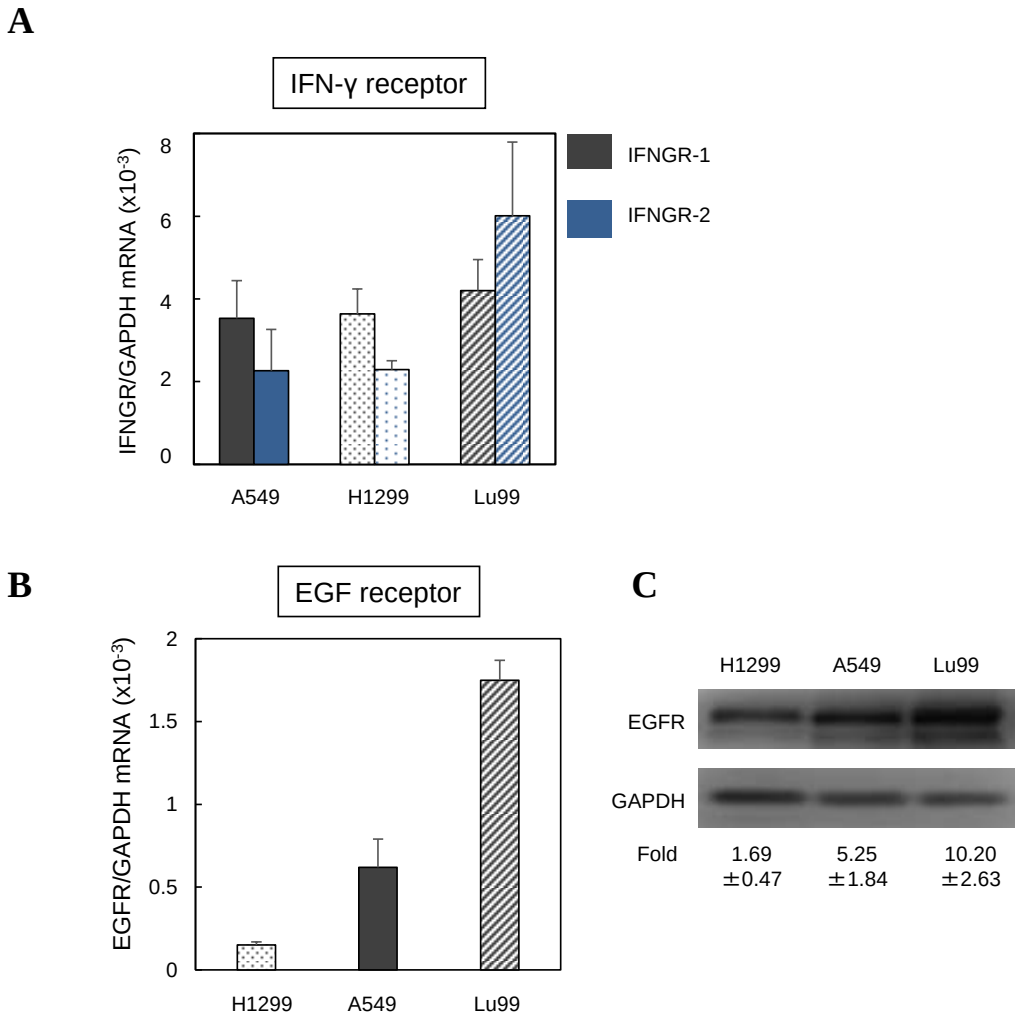

Figure 7. mRNA and protein levels of IFN-γ and EGF receptors expressed in three NSCLC cell lines. (A) IFN-γ receptor 1 (IFNGR1) and IFN-γ receptor 2 (IFNGR2) mRNA expression were examined by qRT-PCR. (B) EGF receptor (EGFR) mRNA levels were examined by qRT-PCR. (C) EGFR protein level was examined by western blotting. Numbers show fold-change ± SD in three different experiments.

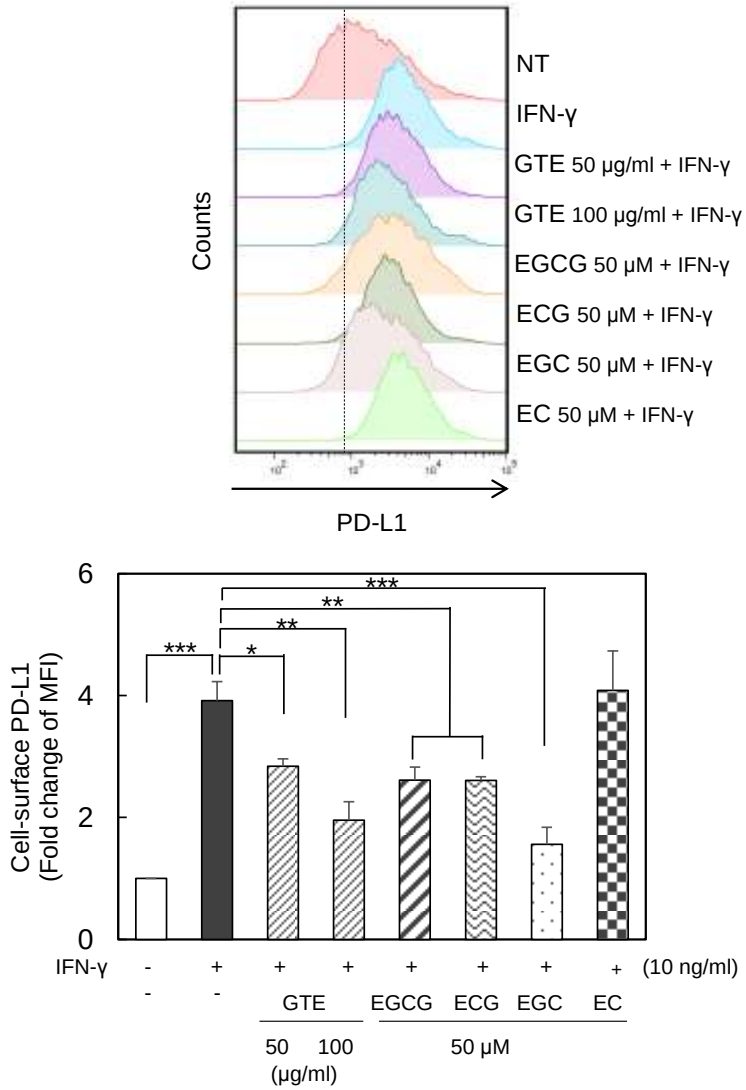

Figure 8. Inhibition of IFN-γ-induced PD-L1 expression with green tea extract (GTE) and green tea catechins in A549 cells. A549 cells were pretreated with 50 and 100 μg/ml GTE or 50 μM of four catechins including EGCG, ECG, EGC and EC for 3 h then treated with 10 ng/ml IFN-γ for 24 h in 1% FBS medium. Cell-surface PD-L1 levels was measured by flow cytometry. The representative histograms are shown in the upper panel. MFI was calculated fold-change of MFI were calculated by comparison with that of non-treated cells. The results show the average ± SD obtained from three independent experiments. *$p < 0.05$, **$p < 0.01$, ***$p < 0.001$ one-way ANOVA using Dunnett's Multiple Comparisons Test.

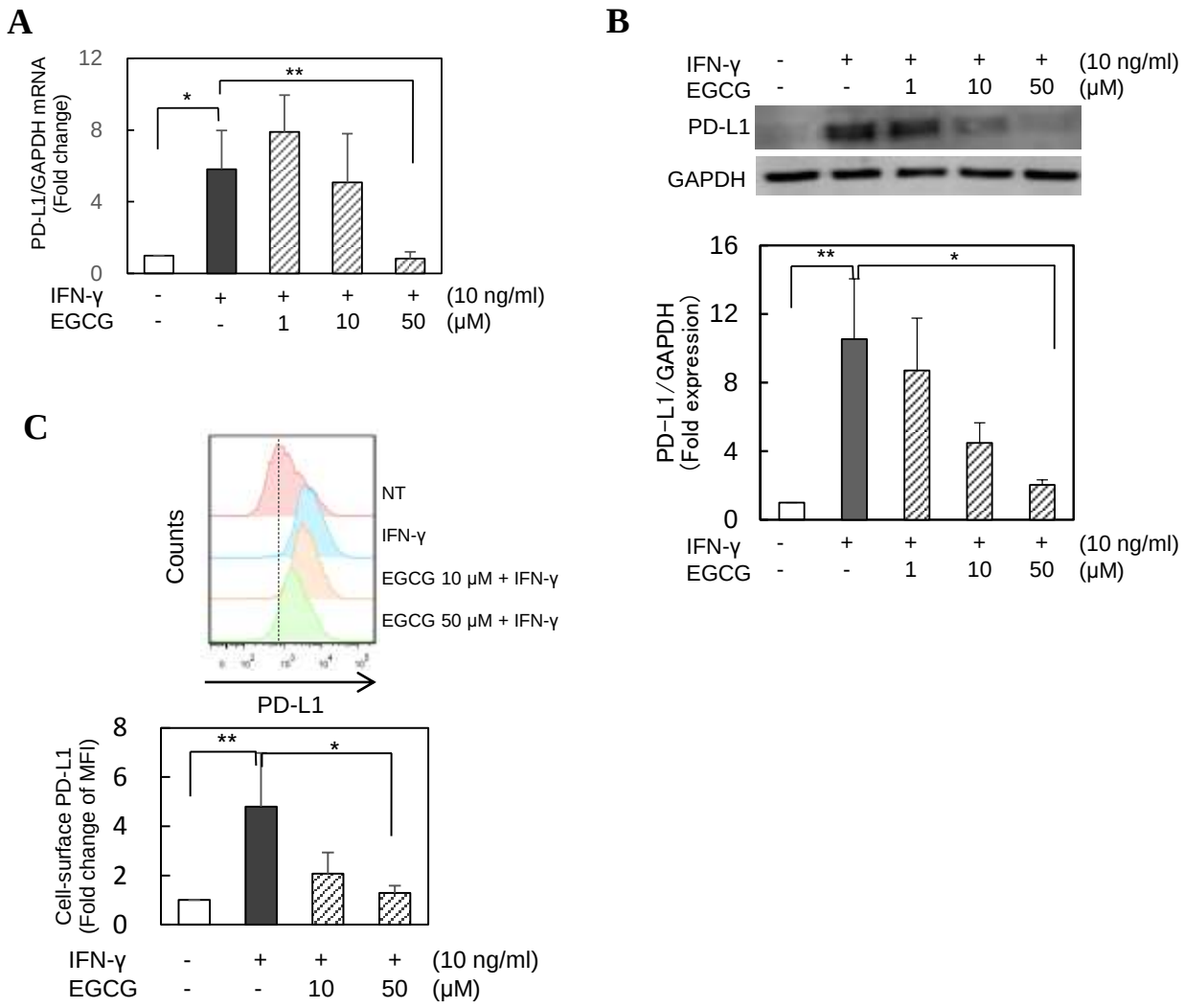

Figure 9. Inhibition of IFN-γ-induced PD-L1 expression with EGCG in A549 cells at the transcription level. A549 cells were pretreated with 1, 10, 50 μM EGCG for 3 h then treated with 10 ng/ml IFN-γ for 24 h in 1% FBS medium. (A) PD-L1 mRNA levels were measured by qRT-PCR. (B) PD-L1 protein levels were examined by western blotting (upper panel) and normalized by GAPDH (lower panel). (C) Cell-surface PD-L1 levels measured by flow cytometry. The representative histograms are shown in the upper panel. Fold-changes of MFI were calculated by comparison with that of non-treated cells (NT). The results show the average ± SD obtained from three independent experiments. *p < 0.05, **p < 0.01 one-way ANOVA using Dunnett's Multiple Comparisons Test.

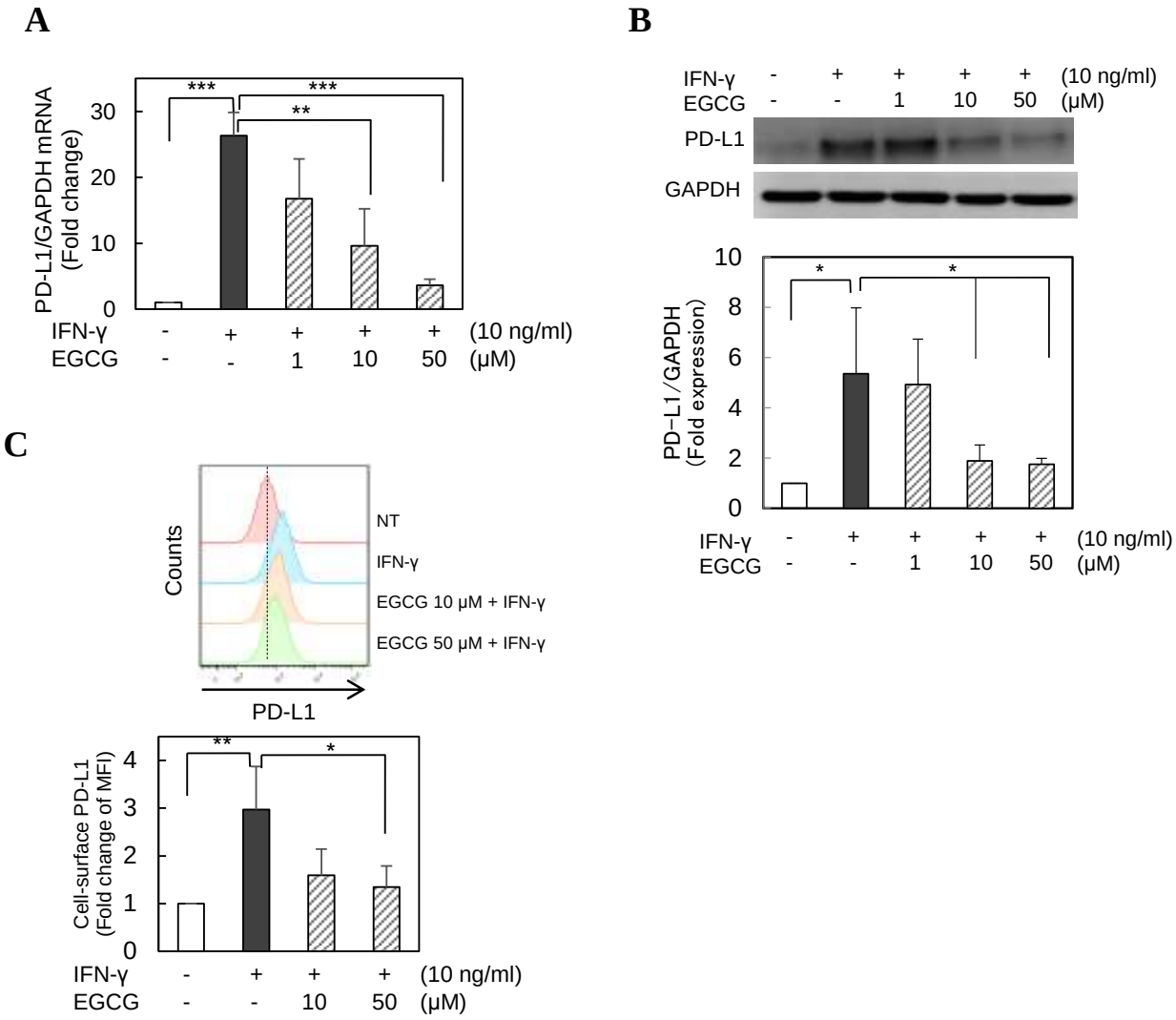

Figure 10. Inhibition of IFN-γ-induced PD-L1 expression with EGCG in H1299 cells at the transcription level. H1299 cells were pretreated with 1, 10, 50 μM EGCG for 3 hrs then treated with 10 ng/ml IFN-γ for 24 h in 1% FBS medium. (A) PD-L1 mRNA levels were measured by qRT-PCR. (B) PD-L1 protein levels were examined by western blotting (upper panel) and normalized by GAPDH (lower panel). (C) Cell-surface PD-L1 levels measured by flow cytometry. The representative histograms are shown in the upper panel. Fold-changes of MFI were calculated by comparison with that of non-treated cells (NT). The results show the average ± SD obtained from three independent experiments. *$p < 0.05$, **$p < 0.01$ one-way ANOVA using Dunnett's Multiple Comparisons Test.

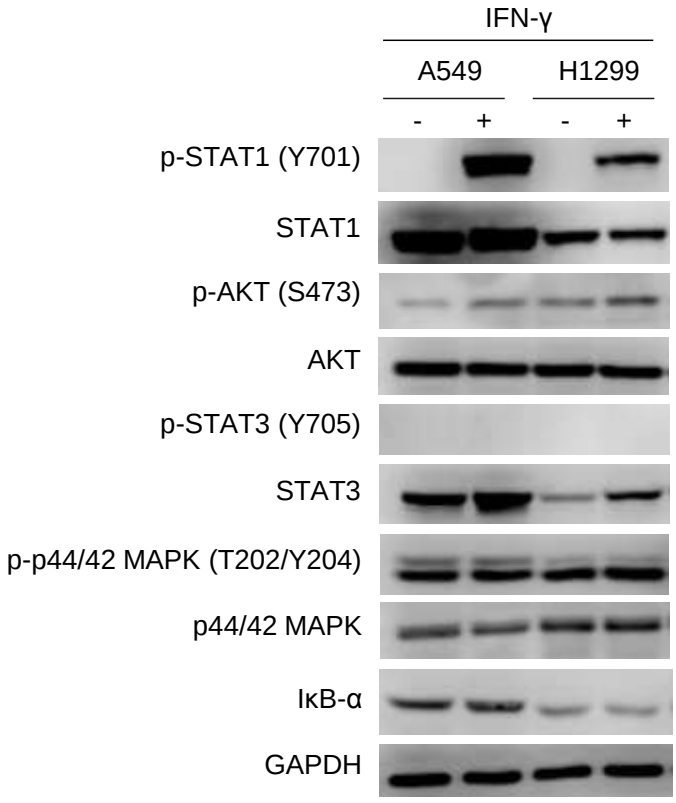

Figure 11. IFN-γ-induced phosphorylation of STAT1. A549 and H1299 cells were treated with 10 ng/ml IFN-γ in 1% FBS medium for 30 min. Effect of IFN-γ on phosphorylation of STAT1, AKT, STAT3, and p42/44 MAPK, or IκB protein level were determined by western blotting using indicated specific antibodies.

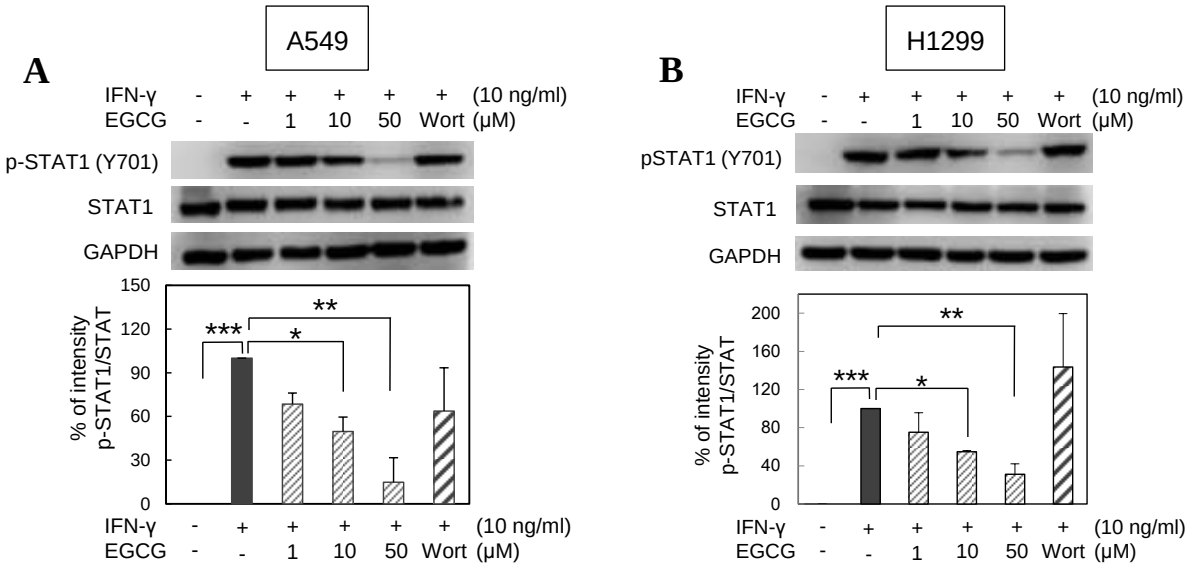

Figure 12. Inhibition of IFN-γ-induced phosphorylation of STAT1 with EGCG in A549 and H1299 cells. A549 and H1299 cells were pretreated with 1, 10, 50 μM EGCG and 1 μM wortmannin, a PI3K inhibitor, for 3 h then treated with 10 ng/ml IFN-γ in 1% FBS medium for 30 min. Phosphorylation of STAT1 at Tyr701 was determined in (A) A549 cells and (B) H1299 cells by western blotting (upper panel), and bar graphs (lower panel) shows average % intensity of phosphorylation of STAT1 versus STAT1 in three independent experiments. GAPDH proteins were shown for internal control. The results show the average ± SD obtained from three independent experiments. *$p < 0.05$, **$p < 0.01$, ***$p < 0.001$ by one-way ANOVA with Dunnett's Multiple Comparisons Test.

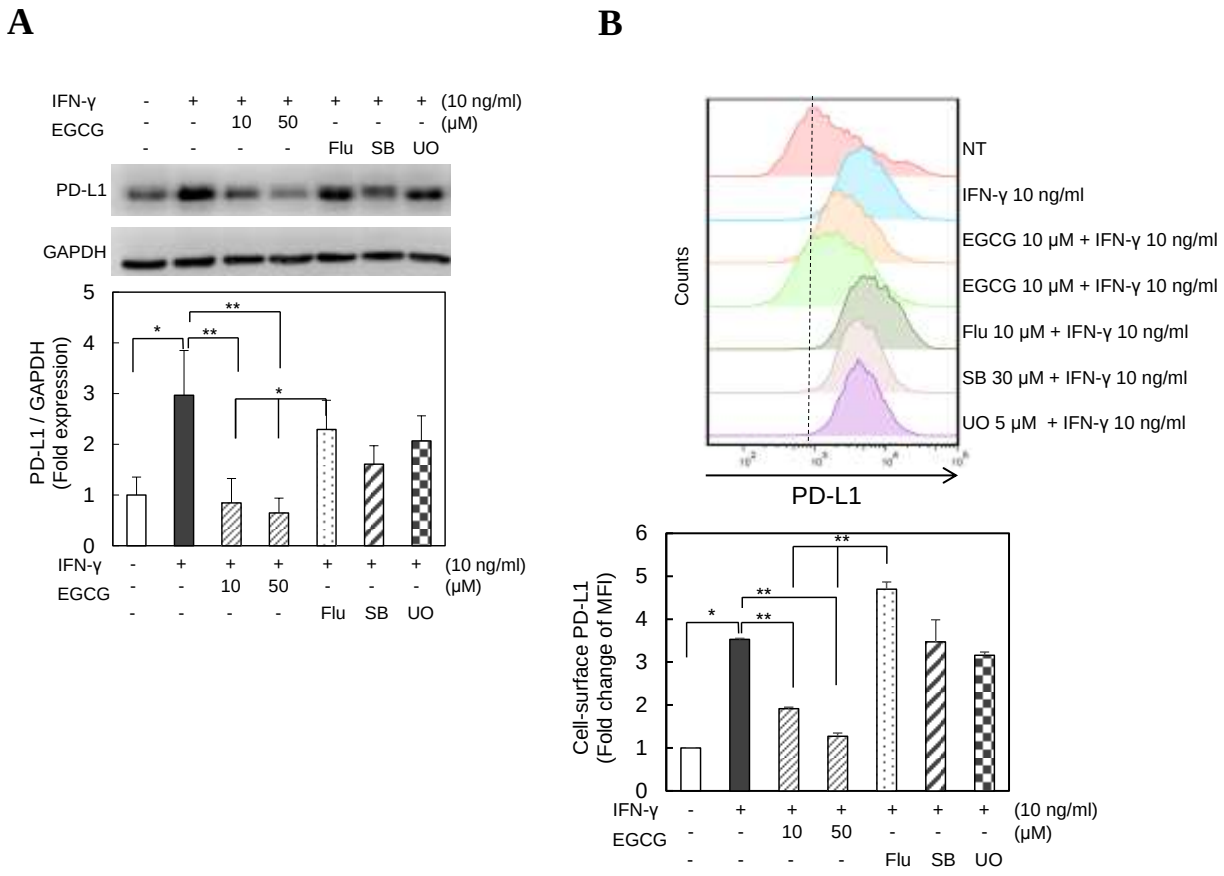

Figure 13. Inhibition of IFN-γ-induced phosphorylation of STAT1 with EGCG stronger than the STAT1 inhibitor. A549 cells were pretreated with 10 and 50 μM EGCG, Flu; 10 μM fludarabine (STAT1 inhibitor), SB: 30 μM SB203580 (p38 MAPK inhibitor), UO: 5 μM UO126 (p44/42 MAPK inhibitor) for 3 h, and then treated with 10 ng/ml IFN-γ for 24 h. (A) PD-L1 protein levels were examined by western blotting (upper panel) and normalized by GAPDH (lower panel). (B) Cell-surface PD-L1 levels were measured by flow cytometry. Fold-changes of MFI were calculated by comparison with that of non-treated cells (NT). The results show the average ± SD obtained from three independent experiments. *$p < 0.05$, **$p < 0.01$, ***$p < 0.001$ one-way ANOVA using Dunnett's Multiple Comparisons Test.

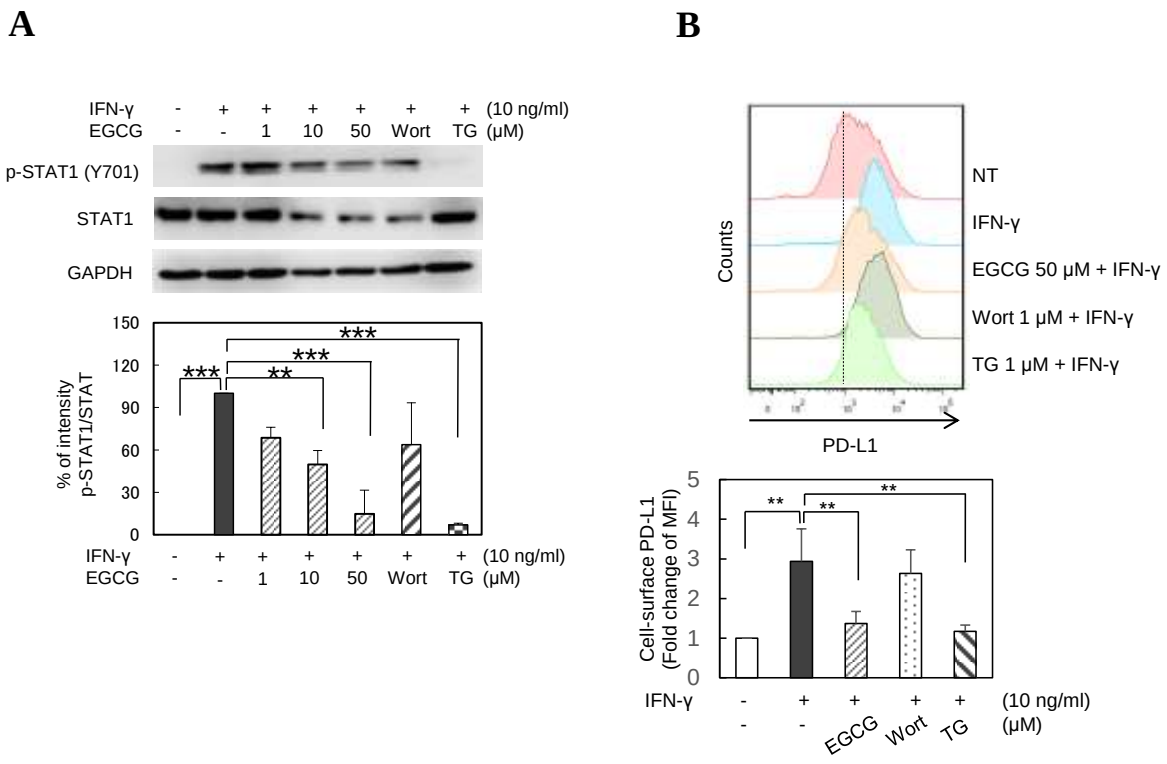

Figure 14. Inhibition of IFN-γ-induced phosphorylation of STAT1 with EGCG similar with JAK2 inhibitor. A549 cells were pretreated with of 1, 10 and 50 μM EGCG, Wort: 1 μM wortmannin (PI3K inhibitor) and TG: 1 μM TG-101348 (JAK2 inhibitor) for 3 hrs, and then treated with 10 ng/ml IFN-γ for 24 h. (A) Phosphorylated of STAT1 and STAT1 protein were examined by western blotting (upper panel), and bar graphs (lower panel) shows the average % intensity of phosphorylation of STAT1 versus STAT1. GAPDH proteins were shown for internal control. (B) Cell-surface PD-L1 levels were measured by flow cytometry. Fold-changes of MFI were calculated by comparison with that of non-treated cells (NT). The results show the average ± SD obtained from three independent experiments. *$p < 0.05$, **$p < 0.01$ one-way ANOVA using Dunnett's Multiple Comparisons Test. NT; non-treated cells

.

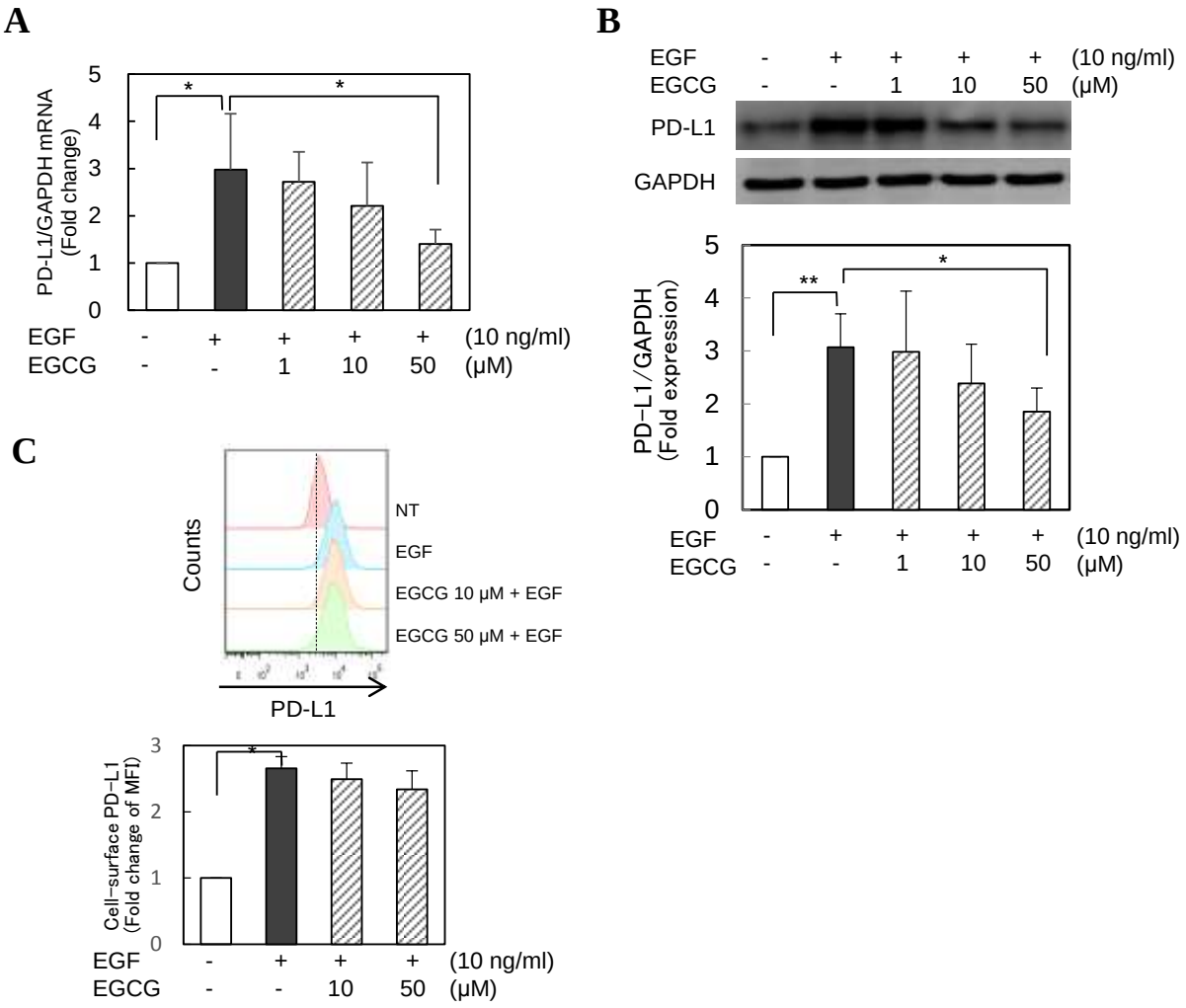

Figure 15. Inhibition of EGF-induced PD-L1 expression with EGCG in Lu99 cells at the transcription level. Lu99 cells were pretreated with 1, 10, 50 μM EGCG for 3 h, and then treated with 10 ng/ml IFN-γ for 24 h. (A) PD-L1 mRNA levels were measured by qRT-PCR. (B) PD-L1 protein levels examined by western blotting (upper panel) and normalized by GAPDH (lower panel). (C) Cell-surface PD-L1 levels measured by flow cytometry. The representative histograms are shown in the upper panel. Fold-changes of MFI were calculated by comparison with that of non-treated cells (NT). The results show the average ± SD obtained from three independent experiments. *$p < 0.05$, **$p < 0.01$ one-way ANOVA using Dunnett's Multiple Comparisons Test.

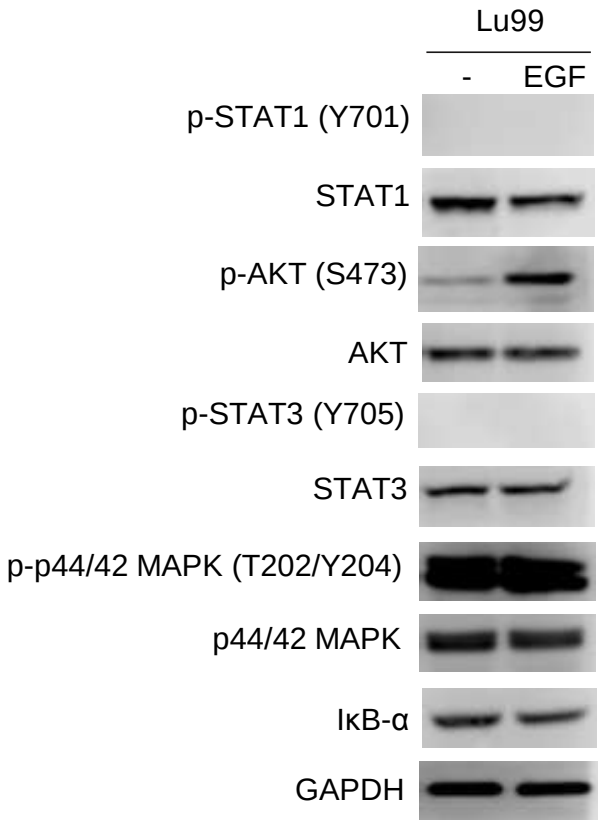

Figure 16. EGF-induced phosphorylation of AKT in Lu99 cells. Lu99 cells were treated with 10 ng/ml EGF for 30 min. Effect of EGF on phosphorylation of STAT1, Akt, STAT3, and p42/44 MAPK, or IκB protein level were determined by western blotting using indicated specific antibodies.

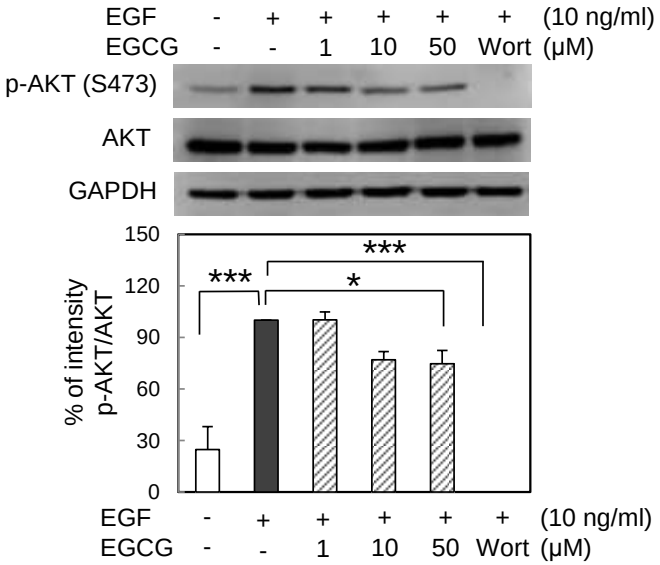

Figure 17. Inhibition of EGF-induced phosphorylation of AKT with EGCG in Lu99 cells. Lu99 cells were pretreated with 1, 10, 50 μM EGCG and 1 μM wortmannin, a PI3K inhibitor, for 3 h, and then treated with 10 ng/ml EGF in 1% FBS medium for 30 min. Phosphorylation of AKT at Ser473 was determined by western blotting (upper panel), and bar graphs (lower panel) shows the average % intensity of phosphorylation of AKT versus AKT in three independent experiments. GAPDH is shown as an internal control. $*p < 0.05$, $**p < 0.01$, $***p < 0.001$ by one-way ANOVA with Dunnett's Multiple Comparisons Test.

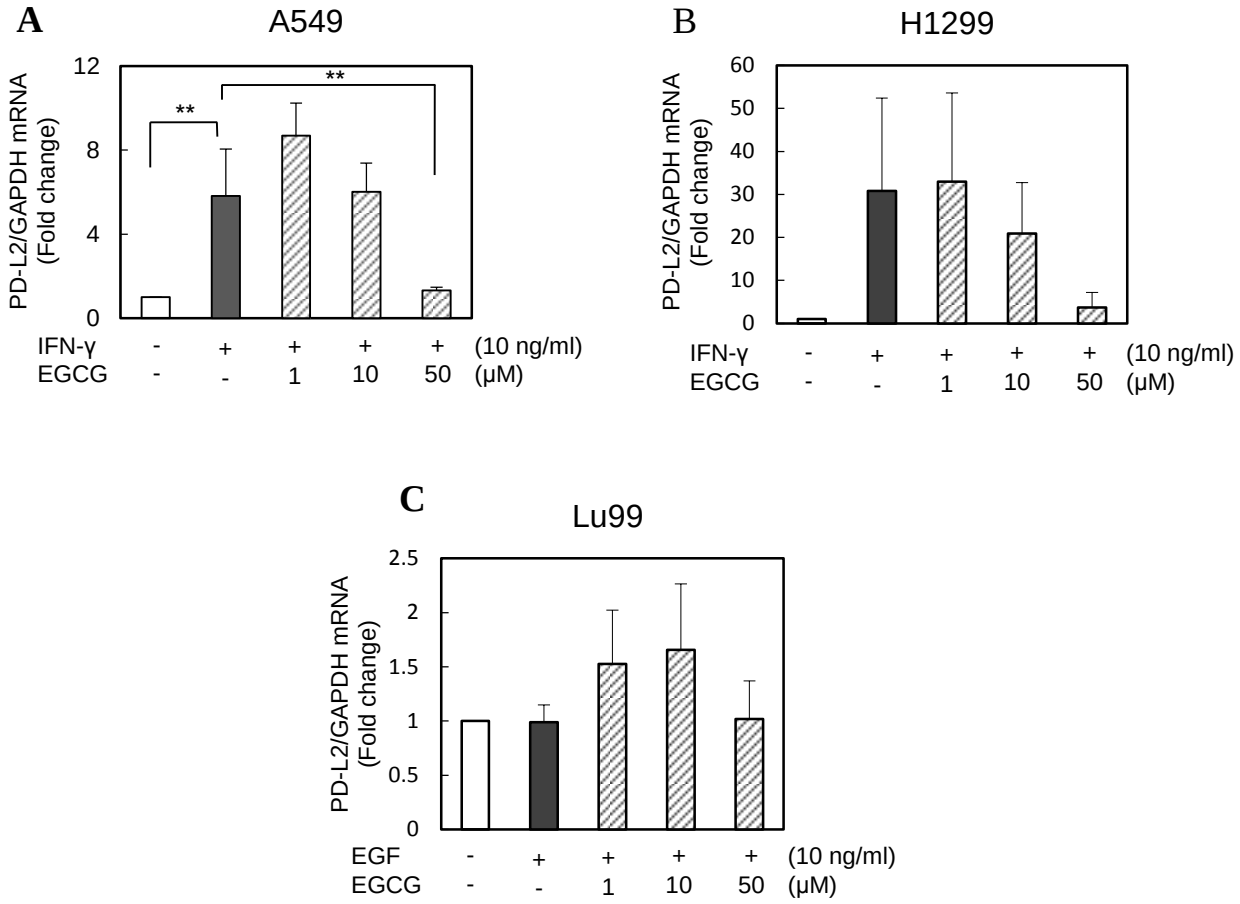

Figure 18. Inhibition of IFN-γ- or EGF-induced PD-L2 mRNA expression with EGCG. After pretreatment with 1, 10, 50 μM EGCG for 3 h. A549, H1299 cells were treated with 10 ng/ml IFN-γ, and Lu99 cells were treated with 10 ng/ml EGF for 24 h. PD-L2 mRNA expression was examined by qRT-PCR in (A) A549 cells, (B) H1299 cells and (C) Lu99 cells. The results show the average ± SD obtained from three independent experiments. $^{**}p < 0.01$ one-way ANOVA using Dunnett's Multiple Comparisons Test.

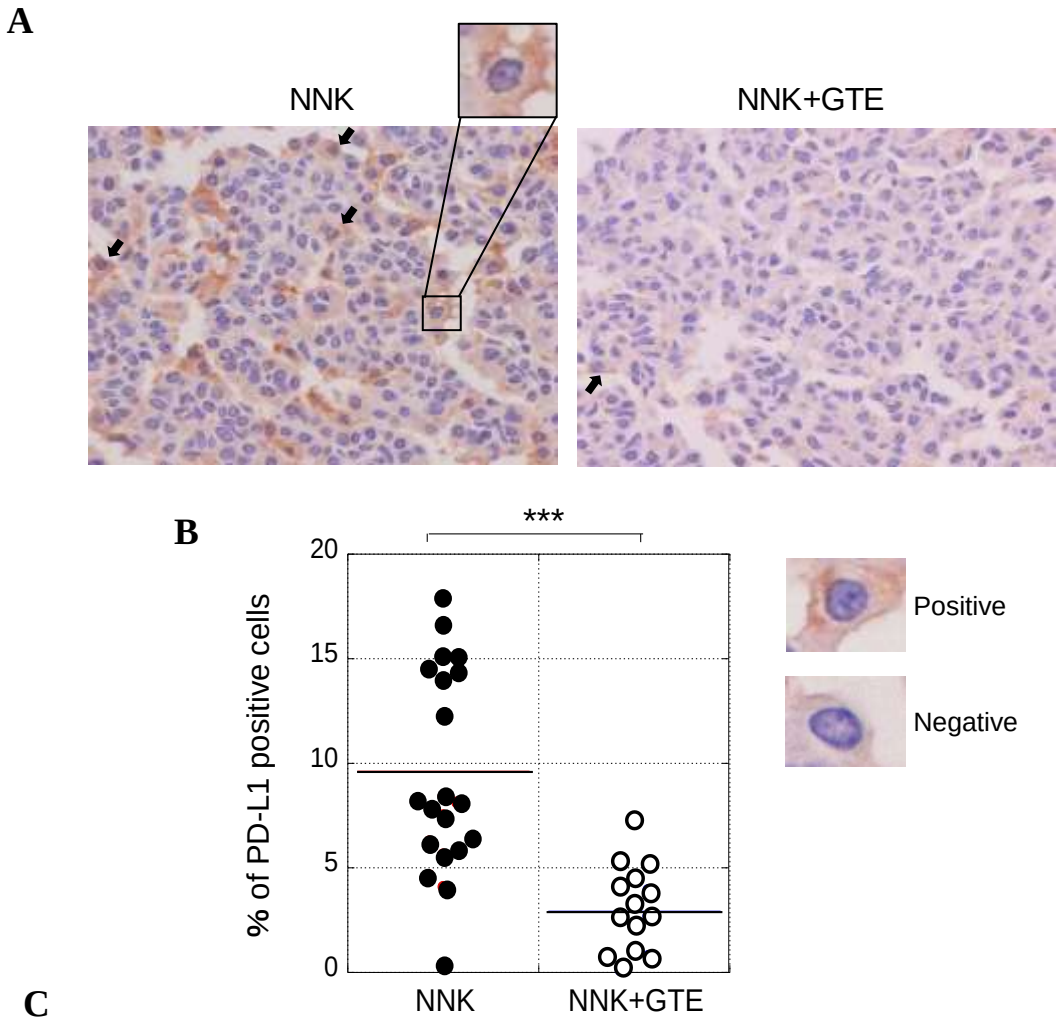

C

Group	Average No. of tumors/mouse ± SE (%)		% of PD-L1 positive cells ± SE (%)	
NNK	4.1 ± 0.5 (100)	*	9.6 ± 4.9 (100)	*
NNK + GTE	2.6 ± 0.4 (63.4)		2.9 ± 2.2 (30.2)	

Figure 19. Oral administration of green tea extract (GTE) inhibits lung tumors of A/J mice induced by NNK and reduces the percentage of PD-L1 positive cells in the tumors. (A) NNK (100 mg/kg body weight) in 100 µL of saline was injected intraperitoneally into two groups of female A/J mice. Two days later, the NNK group continued to receive normal drinking water and the NNK + GTE group received only drinking water with 0.3% GTE for 16 weeks. Lung tumors larger than 0.8 mm in diameter were counted. *$p < 0.05$, analyzed by Student's *t*-test. (A) Representative

immunohistochemical staining of lung tumors with anti-PD-L1 antibody in both NNK and NNK + GTE groups. Black arrows indicate PD-L1 positive cells on the plasma membrane. (B) Percentage of PD-L1 positive cells in individual lung tumors. The symbols ● and ○ indicate the percentage of PD-L1 positive cells in individual tumors in NNK and NNK + GTE groups, respectively. (C) Summary of average No. of tumors/mouse and percent of PD-L1 positive cells. Positive cells were counted independently by three investigators. *$p < 0.05$, analyzed by Wilcoxon-Mann-Whitney test.

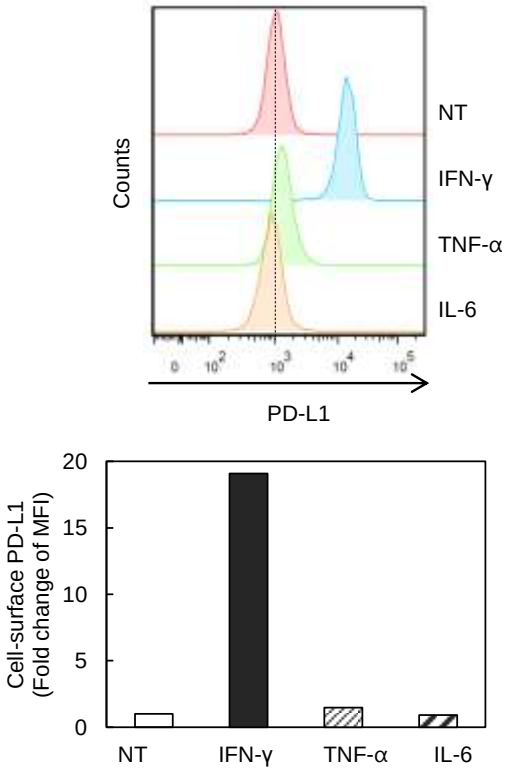

Figure 20. IFN-γ strongly induced cell-surface PD-L1 in B16-F10 cells. Mouse melanoma B16-F10 cells were treated with 50 ng/ml IFN-γ, TNF-α or IL-6 for 24 h. Cell-surface PD-L1 level was examined by flow cytometry. Upper panel shows the representative histograms and the lower panel shows fold-change of or MFI values (lower panel) compared with non-treated-cells (NT).

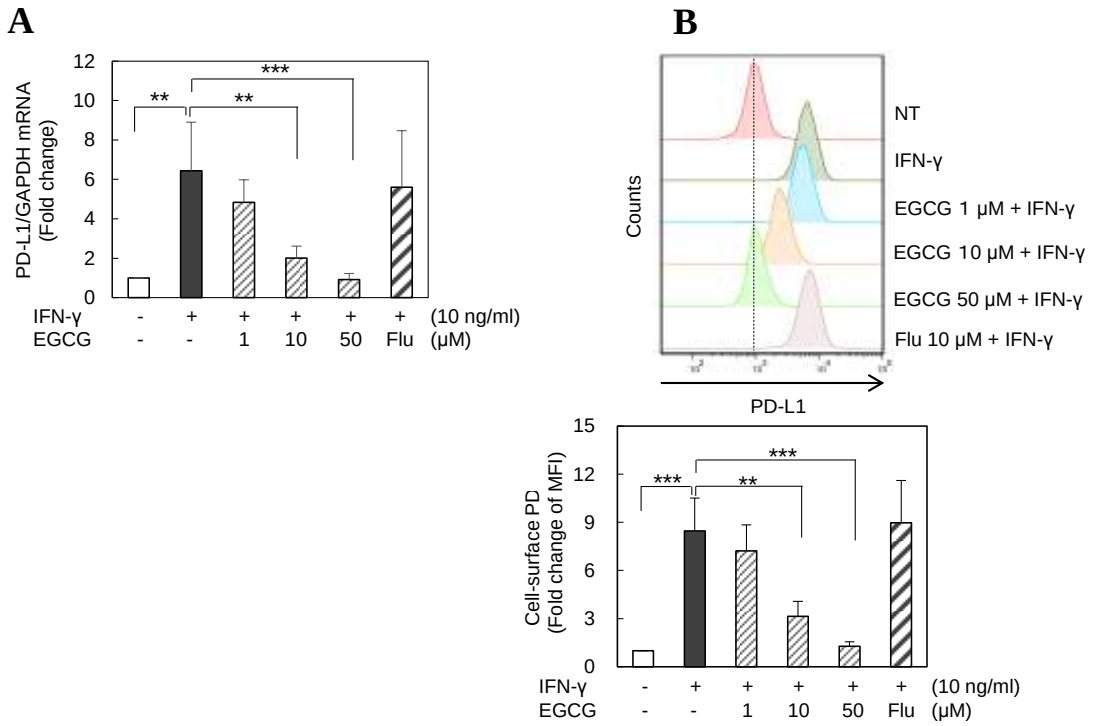

Figure 21. Inhibition of IFN-γ-induced PD-L1 mRNA and protein with EGCG in B16-F10 cells at the transcription level. B16-F10 cells were pretreated with 1, 10, 50 μM EGCG or 10 μM fludarabine, a STAT1 inhibitor; Flu, for 3 h, and then treated with 10 ng/ml IFN-γ for 24 h. (A) PD-L1 mRNA expression was examined by qRT-PCR. (B) Cell-surface PD-L1 levels measured by flow cytometry. The representative histograms are shown in the upper panel. Fold-changes of MFI were calculated by comparison with that of non-treated cells (NT). The results show the average ± SD obtained from three independent experiments. $^{**}p < 0.01$, $^{***}p < 0.001$ one-way ANOVA using Dunnett's Multiple Comparisons Test.

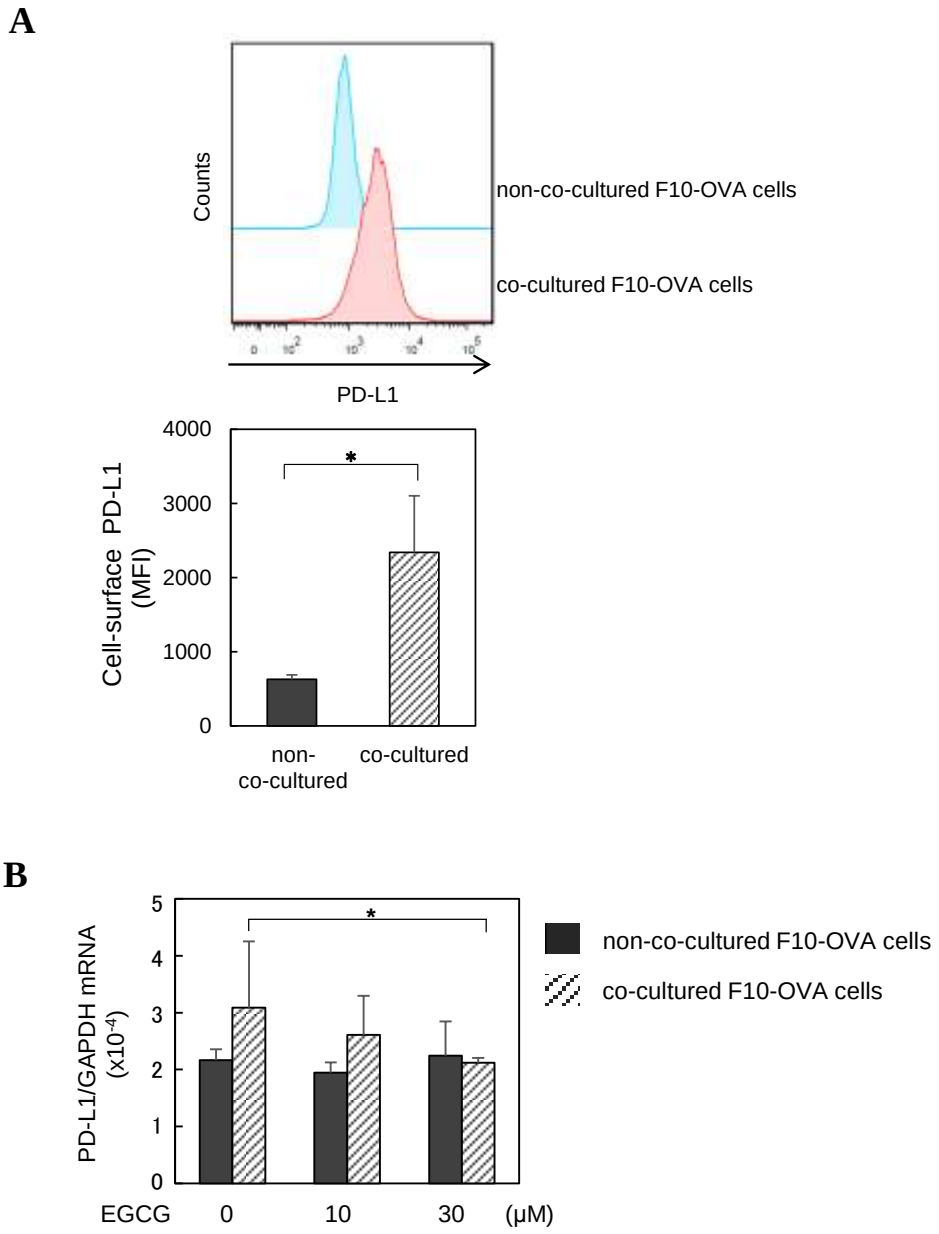

Figure 22. EGCG inhibits PD-L1 mRNA induced by co-cultured with tumor specific T cells. CD3+ T cells were isolated from immunized mice with mitomycin C treated F10-OVA cells as described in Materials and Methods. Mitomycin C-treated F10-OVA cells (2×10^5 cells) were co-cultured with tumor specific CD3+ T cells (2×10^6 cells) for 48 h. (A) Cell-surface PD-L1 were measured by flow cytometry compared with non-co-cultured F10-OVA cells. The representative histograms are shown in the upper panel and average MFI values are shown in the lower panel. (B) PD-L1 mRNA were examined by qRT-PCR. The results show the average ± SD of three independent experiments. *p < 0.05, one-way ANOVA using Dunnett's Multiple Comparisons Test.

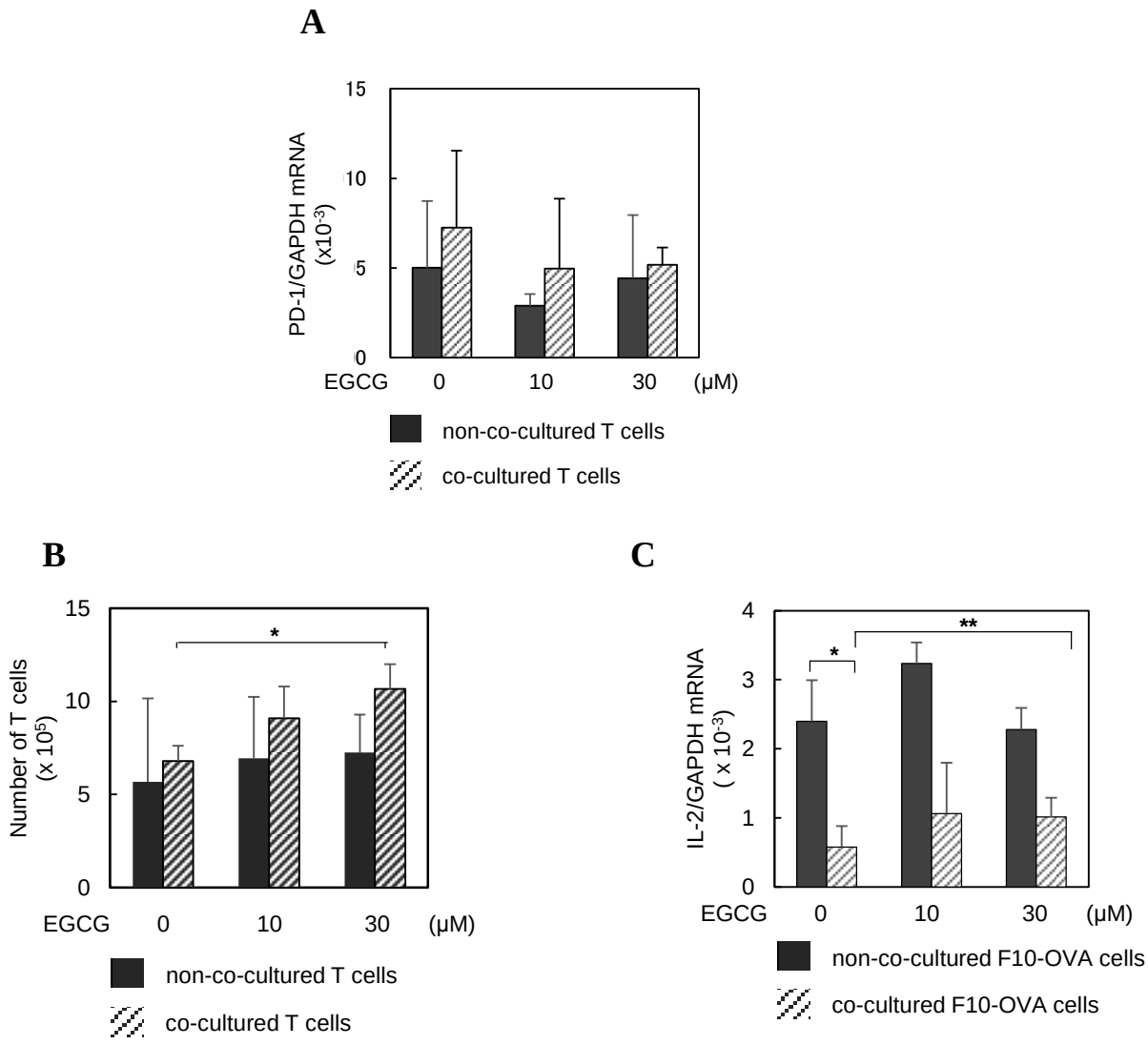

Figure 23. EGCG restored IL-2 mRNA expression in tumor specific CD3+ T cells co-cultured with F10-OVA cells. Mitomycin C-treated F10-OVA cells were pretreatment with EGCG for 3 h in 10% FBS co-culture medium. Tumor specific CD3+ T cells (2 x 10^6 cells) were added to F10-OVA cells (2 x 10^5 cells) and co-cultured for 48 h. (A) PD-1 mRNA expression was examined by qRT-PCR. (B) The number of T cells were counted by trypan blue exclusion method. (C) IL-2 mRNA expression was examined by qRT-PCR. The results show the average ± SD of three independent experiments. *$p < 0.05$, **$p < 0.01$ one-way ANOVA using Dunnett's Multiple Comparisons Test.

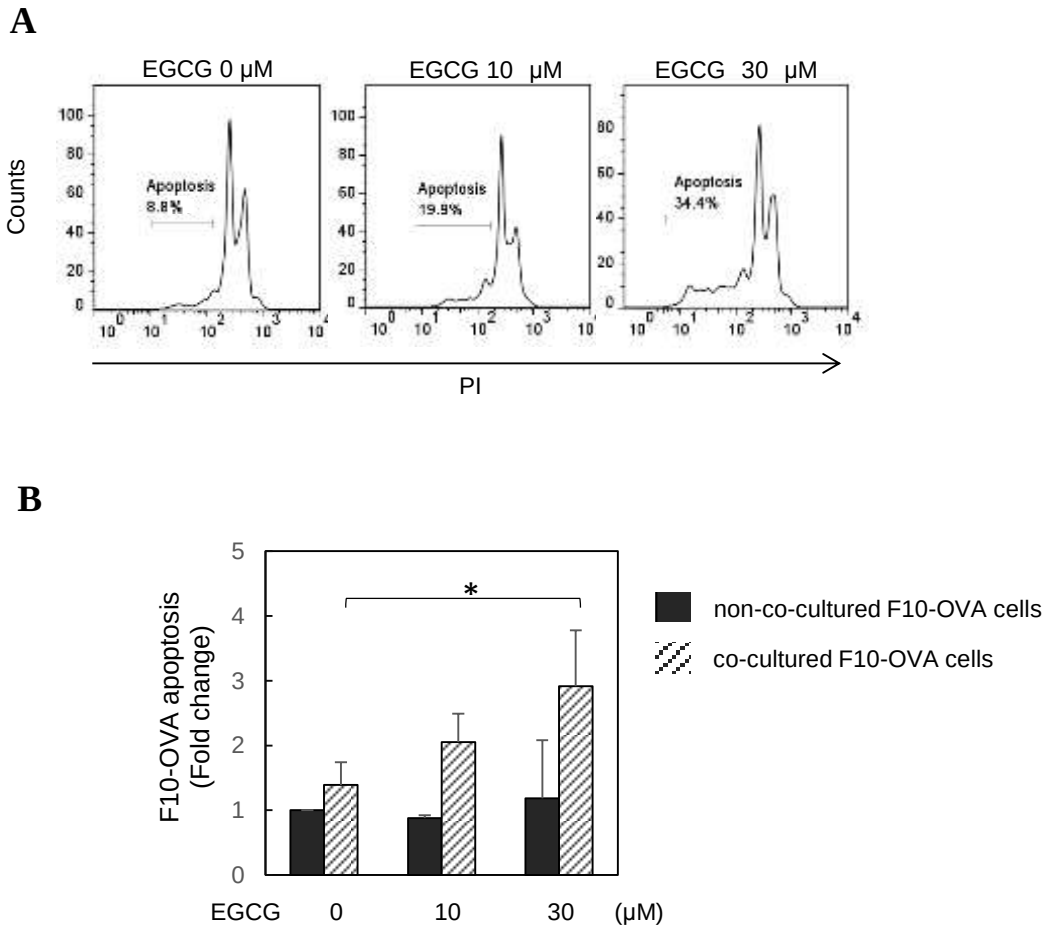

Figure 24. EGCG stimulated apoptosis in F10-OVA cells by co-cultured with tumor specific CD3+ T cells. Mitomycin C-treated F10-OVA cells were pretreatment with EGCG for 3 h in 10% FBS co-culture medium. Tumor specific CD3+ T cells (2 x 10^6 cells) were added to F10-OVA cells (2 x 10^5 cells) and co-cultured for 48 h. (A) The representative results of flow cytometry. Percent sub-G1 phase cells indicate % of apoptosis cells. (B) Fold-change of apoptosis cells were shown in the graph. The results show the average ± SD of three independent experiments. *$p < 0.05$, one-way ANOVA using Dunnett's Multiple Comparisons Test.

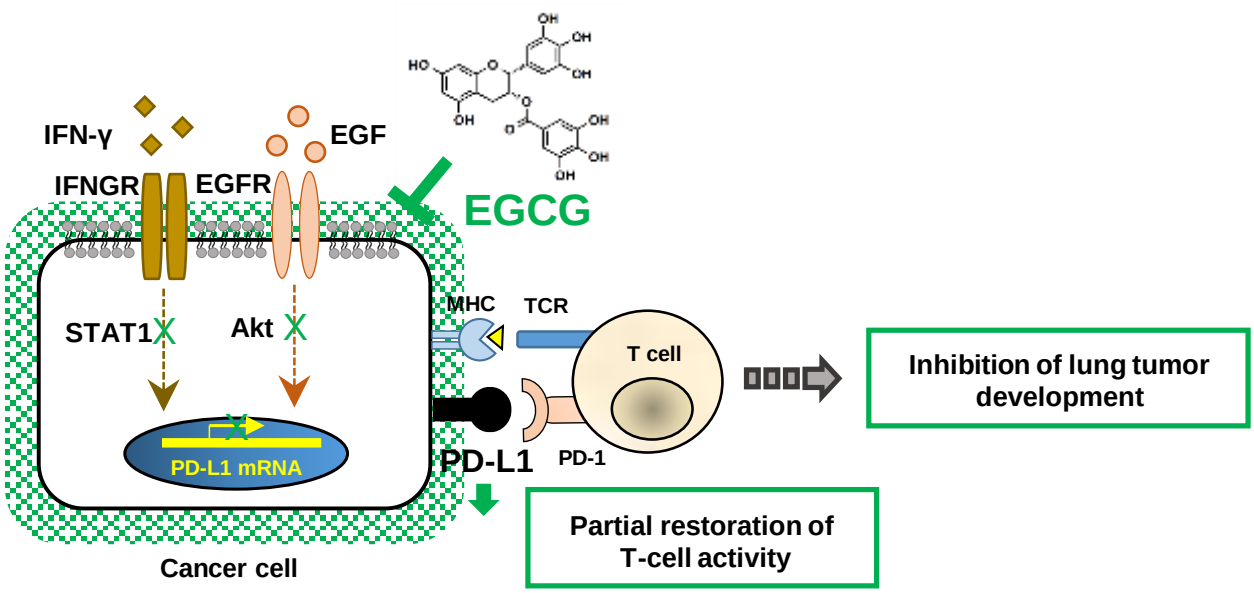

Figure 25. A schematic illustration of EGCG restores T-cell activity by inhibition of PD-L1 expression, resulting in inhibition of lung tumor development.

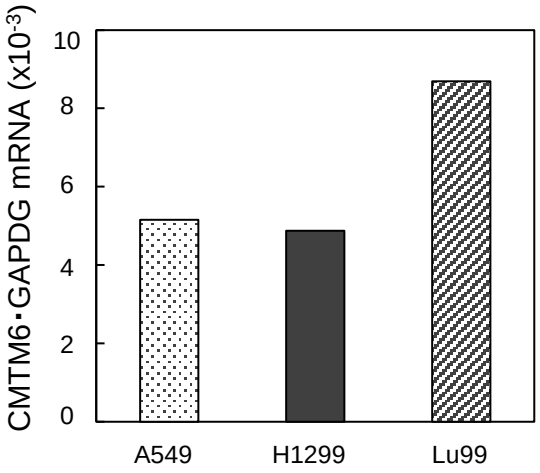

Supplemental Figure 1. Lu99 cells maintained high CKLF Like MARVEL Transmembrane Domain Containing 6 (CMTM6) mRNA expression. The CMTM6 mRNA level of A549, H1299, and Lu99 cells were analyzed by qRT-PCR.